Title

Analysis of Traffic Flow With Mixed Manual and Intelligent Cruise Control Vehicles: Theory and Experiments

Authors

Bose, Arnab
Ioannou, Petros

Publication Date

2001-04-01

CALIFORNIA PATH PROGRAM
INSTITUTE OF TRANSPORTATION STUDIES
UNIVERSITY OF CALIFORNIA, BERKELEY

Analysis of Traffic Flow With Mixed Manual and Intelligent Cruise Control Vehicles: Theory and Experiments

Arnab Bose, Petros Ioannou
University of Southern California

California PATH Research Report
UCB-ITS-PRR-2001-13

This work was performed as part of the California PATH Program of the University of California, in cooperation with the State of California Business, Transportation, and Housing Agency, Department of Transportation; and the United States Department of Transportation, Federal Highway Administration.

Report for MOU 392

April 2001

ISSN 1055-1425

ANALYSIS OF TRAFFIC FLOW WITH MIXED MANUAL AND INTELLIGENT CRUISE CONTROL VEHICLES: THEORY AND EXPERIMENTS*

Arnab Bose and Petros Ioannou

Center for Advanced Transportation Technologies

Dept. of Electrical Engineering-Systems, EEB200A

University of Southern California

Los Angeles, CA 90089-2562, USA

abose@usc.edu, ioannou@almaak.usc.edu

* This work is supported by the California Department of Transportation through PATH of the University of California. The contents of this report reflect the views of the authors who are responsible for the facts and accuracy of the data presented herein. The contents do not necessarily reflect the official views or policies of the State of California or the Federal Highway Administration. This report does not constitute a standard, specification or regulation.

ANALYSIS OF TRAFFIC FLOW WITH MIXED MANUAL AND INTELLIGENT CRUISE CONTROL VEHICLES: THEORY AND EXPERIMENTS

Arnab Bose and Petros Ioannou

Abstract

During the last decade considerable research and development efforts have been devoted to automating vehicles in an effort to improve safety and efficiency of vehicular traffic. While dedicated highways with fully automated vehicles is a future objective, the introduction of Intelligent Cruise Control (ICC) vehicles on current highways designed to operate with manually driven vehicles is a realistic near term objective. The purpose of this report is to analyze the effects on traffic flow characteristics and environment when ICC vehicles with automatic vehicle following capability (in the same lane) operate together with manually driven vehicles. We have shown that ICC vehicles do not contribute to the slinky effect phenomenon observed in today's highway traffic when the lead manual vehicle performs smooth acceleration maneuvers. We have demonstrated that ICC vehicles help smooth traffic flow by filtering the response of rapidly accelerating lead vehicles. The accurate speed tracking and the smooth response of the ICC vehicles designed for passenger comfort reduces fuel consumption and levels of pollutants of following vehicles. This reduction is significant when the lead manual vehicle performs rapid acceleration maneuvers. We have demonstrated using simulations that the fuel consumption and pollution levels present in manual traffic simulated using a car following model that models the slinky effect behavior observed in manual driving can be reduced during rapid acceleration transients by 28.5% and 1.5%-60.6% respectively due to the presence of 10% ICC vehicles. These environmental benefits are obtained without any adverse effects on the traffic flow rates. Experiments with actual vehicles are used to validate the theoretical and simulation results.

Keywords: Intelligent Cruise Control (ICC) vehicles, manually driven (manual) vehicles, mixed traffic, slinky-type effects, pollution emission, fuel consumption.

Executive Summary

In this report the effects of ICC vehicles among manual ones are analyzed, simulated and experimentally investigated using actual vehicles. We show that the ICC vehicles do not contribute to the slinky-type effects during smooth transients. In the presence of rapid transients, the ICC vehicles act as filters and convert the rapid transients into smooth ones, thereby smoothing traffic flow. Furthermore, our analysis shows that the smoothing characteristic of the ICC vehicles is not at the expense of traffic flow. These characteristics have beneficial environmental implications that are significant during rapid acceleration transients. The theoretical and simulation findings have been validated using experiments with actual vehicles.

Contents

List of Figures

List of Tables

1 Introduction

Recent advances in technology have propelled efforts to automate vehicles in order to achieve safe and efficient use of the current highway system. Fully automated vehicles that are able to operate in a highway environment are a long-term goal. On the other hand, partially or semi-automated vehicles designed to operate with current manually driven vehicles in today's highway traffic are seen as a more near term objective. Their gradual penetration into the current highway system will usher the stage of mixed traffic where semi-automated vehicles will coexist with manually driven ones.

Considering the current penetration of products such as Anti-Lock Braking Systems (ABS), air bags and cruise control into the vehicle market, it is justifiable to expect that Intelligent Cruise Control (ICC) systems[1] that give vehicles the capability to follow each other automatically in the same lane, will be deployed in the US in the near future and penetrate the market in a similar fashion. Several major car manufacturers in Japan are already producing vehicles for sale with an ICC option. ICC is the next step to cruise control. It allows a vehicle to automatically follow another vehicle in a single lane using automatic throttle and brake controllers [1] in conjunction with various on-board sensors [15]. We refer to vehicles with ICC capability as ICC vehicles since they provide automation only in the longitudinal direction [2]. The driver is still responsible for lateral control of the ICC vehicle. In the initial stages, ICC systems may be designed, as a driver assist device and the driver will be responsible for crucial tasks like collision avoidance. Such a system may require the use of a fairly large vehicle spacing (compared to the average used in today's driving) in an effort to account for possible larger driver reaction times due to the use of automation. As drivers become accustomed to the system and human factors and technical issues are resolved, ICC systems could be upgraded to have a longitudinal frontal collision avoidance (FCA) system [3]. In that case the vehicle spacing could be reduced considerably which could result into significant improvements in highway capacity.

Human factor considerations dictate that the response of an ICC vehicle should be smooth. As a result an ICC vehicle is expected to act as a filter in vehicle following attenuating disturbances and smoothing traffic flow. Meanwhile, the vehicle-highway system is one of the major contributors to air pollution in urban areas due to increasing vehicle miles traveled and congestion [5]. With the gradual penetration of ICC vehicles into manual traffic, the question is whether the different dynamical response of ICC vehicles will have any impact on the environment and characteristics of traffic flow.

In this report we examine the effect of ICC vehicles on the transient behavior of traffic flow at the microscopic level when they operate together with manually driven vehicles. In our analysis we consider a human driver car following model [8,9] and a model of an ICC vehicle [1]. These models are used to analyze the transient behavior during vehicle

[1] ICC is often referred to as Adaptive Cruise Control (ACC). The name ACC is also used by some vehicle manufacturers to refer to the cruise control system that employs adaptive control. For this reason in this report as in previous publications we continue to use the name ICC.

following for three different cases. In case 1 all vehicles are manually driven. In case 2 all vehicles are ICC and in case 3 manual and ICC vehicles are mixed.

We have shown that in manual driving, a car following model namely Pipes model [8,9] models slinky-type effects [6], a phenomenon observed in today's traffic. Thus, we use the Pipes model to simulate manual vehicle dynamics and examine the effect of mixing manually driven and ICC vehicles on the traffic flow characteristics during transients. Moreover, the response of the Pipes model is compared to actual manual vehicle responses involving different drivers. It is observed that slinky-type effects are more pronounced in actual manual driving than that modeled by the Pipes model. On the other hand, the ICC vehicle is modeled using an ICC design developed in [1] that is free of slinky-type effects and is designed to provide smooth driving at all times with the exception of emergencies.

Our analysis with mixed traffic shows that a "smooth" acceleration maneuver exhibited by a lead vehicle propagates upstream and gets amplified leading to the slinky effect phenomenon. In this case the ICC vehicles do not contribute to the slinky effect since they are designed to respond to any smooth acceleration/velocity response in an accurate manner. When the lead vehicle exhibits a "rough" acceleration maneuver the ICC vehicle in a mixed traffic situation acts as a filter by converting the "rough" acceleration response to a smooth response in an effort to maintain smooth driving. This is done at the expense of larger position, velocity and acceleration errors and sometimes at the expense of falling far behind the vehicle ahead. We have shown that these characteristics of the ICC vehicles have a very beneficial effect on fuel economy and pollution, which is significant during rapid acceleration transients. Simulations are used to quantify these benefits using the Pipes model [8,9] and the ICC model developed in [1]. We demonstrate that the fuel consumption and pollution levels present in manual traffic can be reduced during smooth acceleration maneuvers by 8.5% and 8.1%-18.4% respectively, and during rapid acceleration transients by 28.5% and 1.5%-60.6% respectively, due to the presence of 10% ICC vehicles. It is demonstrated that these environmental benefits are obtained without any adverse effects on the traffic flow rate.

The quantitative benefits obtained using simulations were validated by experiments using 3 manually driven and ICC vehicles. The simulation results were repeated for the 3 vehicles modeled by the Pipes model and the ICC model using exactly the same driving scenarios as in the experiments. The comparison shows that the experiments validate the simulation results. Our analysis also indicates that the environmental benefits obtained in mixed traffic during vehicle transient responses are not at the expense of traffic flow rates.

The report is organized as follows. In Section 2 we outline the concept of string stability in vehicle following and in Sections 3 and 4 we analyze human driver car following and ICC vehicle models for string stability, respectively. We then extend our analysis into the case of mixed manual/ICC vehicles in Section 5. In Section 6 we perform simulations for different car following scenarios in manual and mixed traffic and confirm the analytical findings. In this Section we also compare the responses of the Pipes model with that of an

actual manually driven vehicle. In Section 7 we discuss the environmental results using simulations and experiments with actual vehicles. In Section 8 we examine the effect of traffic disturbances due to rapid vehicle acceleration transients on mixed traffic flow. We present our conclusions in Section 9.

2 String Stability: Mathematical Definitions

In vehicle following the dynamics of each vehicle are coupled with other vehicles leading to a larger dynamical system. Even though each vehicle may have stable behavior and good performance, the behavior of the overall coupled system may not be desirable. For example, transients caused by a single vehicle changing its speed may be amplified upstream leading to what is known as "slinky-type effect" [6] or string instability. String stability [17] in vehicle following implies that any nonzero position, velocity and acceleration error of an individual vehicle in a string of vehicles does not get amplified as it propagates upstream. We begin by giving the mathematical definitions of string stability for interconnected systems of vehicles closely following each other in a single lane. Next, microscopic human driver car following and ICC vehicle models are used to investigate string stability in manual, ICC vehicular and mixed traffic situations. Finally, we perform a series of simulations to illustrate different manual and mixed traffic vehicle following scenarios.

A system of vehicles in a single lane under moderately dense traffic conditions can be considered as a countable infinite interconnected system. For simplicity, i.e. to avoid boundary conditions, we consider the system to consist of infinite subsystems. If a system comprises of finite number of subsystems, it can be treated as if the number were infinite by assuming fictitious subsystems at both ends. Such a system shown in Fig. 1 can be modeled as [18]

$$v_i = G_i(s)v_{i-1} \tag{1}$$

where $i \in N$, and N is the number of vehicles considered, v_i is the longitudinal speed of the ith vehicle and $G_i(s)$ is a proper stable transfer function that represents the input-output dynamics of the ith vehicle in the longitudinal direction. The system represents traffic in a single lane without passing in which every vehicle tries to match the speed of the preceding vehicle with some precision and vehicle spacing. The details of the dynamics of such a system are often described by complex nonlinear dynamical models. Such models are linearized about an operating speed to put them in the framework of (1), without affecting the accuracy of the response within the operating range of interest.

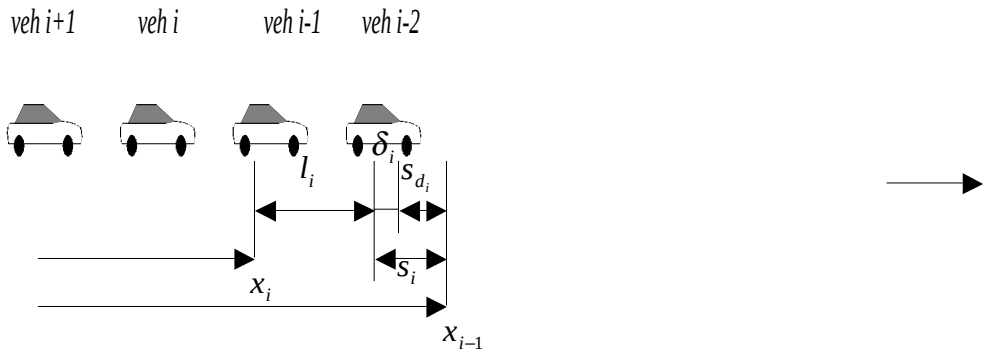

Figure 1: Interconnected system of vehicles following each other in a single lane.

Definition 1 (Class of interconnected systems): The class of interconnected systems consists of interconnected systems that satisfy (1).

Let us define the following errors for the *i*th vehicle as depicted in Figure 1:

$$\delta_i = s_i - s_{d_i} = x_{i-1} - x_i - l_i - s_{d_i} \qquad \text{(position error)}$$

$$v_{ri} = v_{i-1} - v_i \qquad \text{(velocity error)}$$

$$a_{ri} = a_{i-1} - a_i \qquad \text{(acceleration error)}$$

where x_i denotes the abscissa of the rear bumper of the *i*th vehicle

s_{d_i} is the desired intervehicle spacing to be followed by the *i*th vehicle

s_i is the actual intervehicle spacing measured from the rear of the *i*-1 vehicle to the front of the *i*th vehicle

l_i is the length of the *i*th vehicle

δ_i denotes the deviation between the actual and the desired intervehicle spacing, also referred to as the position error

v_i denotes the velocity of the *i*th vehicle

a_i denotes the acceleration of the *i*th vehicle

Definition 2 (String Stability): The interconnected system of vehicles given in (1) is *string stable* if the position, velocity and acceleration errors do not amplify when they propagate upstream, i.e.

$$\begin{aligned} &\|\delta_i\|_p \le \|\delta_{i-1}\|_p \\ &\|v_{ri}\|_p \le \|v_{ri-1}\|_p \qquad \forall p \in [1,\infty],\ \forall \quad i \in N \\ &\|a_{ri}\|_p \le \|a_{ri-1}\|_p \end{aligned} \qquad (2)$$

Definition 3 (Strict String Stability): The interconnected system of vehicles given in (1) is *strictly string stable* if the position, velocity and acceleration errors attenuate when they propagate upstream, i.e.

$$\begin{aligned} &\|\delta_i\|_p < \|\delta_{i-1}\|_p \\ &\|v_{ri}\|_p < \|v_{ri-1}\|_p \qquad \forall\, p \in [1,\infty],\ \forall \quad i \in N \\ &\|a_{ri}\|_p < \|a_{ri-1}\|_p \end{aligned} \tag{3}$$

Definition 4 (String Unstable): The interconnected system of vehicles given in (1) is said to be *string unstable* if it does not satisfy (2) for any $i \in N$ or for any $p \in [1,\infty]$.

Case 1: Vehicles with constant desired intervehicle spacing

Let us consider the case where the desired intervehicle spacing s_{d_i} is constant at all speeds. Consider a string of vehicles with different transfer functions $G_i(s)$ that satisfy (1). We have

$$\delta_i = x_{i-1} - x_i - l_i - s_{d_i}$$

$$\delta_i = \frac{1}{s}[v_{i-1} - v_i] - l_i - s_{d_i}$$

where '*s*' is the Laplace operator.

For string stability analysis we focus on the upstream propagation of transient position/velocity/acceleration errors. During such transients, we have $sl_i = ss_{d_i} = 0$ for constant vehicle length l_i and constant intervehicle spacing s_{d_i}. Thus, neglecting these non-contributing terms since they have no effect on the transient position error analysis, we have

$$\delta_i = \frac{1}{s}(1 - G_i)v_{i-1}$$

$$v_{ri} = v_{i-1} - v_i = (1 - G_i)v_{i-1}$$

$$a_{ri} = \dot{v}_{ri} = \dot{v}_{i-1} - \dot{v}_i$$

or,

$$a_{ri} = s(1 - G_i)v_{i-1}$$

which shows that

$$\frac{\delta_i}{\delta_{i-1}} = \frac{v_{ri}}{v_{ri-1}} = \frac{a_{ri}}{a_{ri-1}} = \frac{(1-G_i)}{(1-G_{i-1})} G_{i-1} = \overline{G_i}(s) \qquad (4)$$

Remark 1: When all the vehicles have identical input-output characteristics, i.e. $G_i(s) = G(s)$, then $\overline{G_i}(s) = G(s)$.

Instead of the constant intervehicle spacing policy, we may have vehicles with constant time headway policy, in which case the desired intervehicle spacing is proportional to the vehicle speed and the proportionality constant is known as the time headway. Time headway is defined as the time it takes for a vehicle to cover the distance measured from the rear of the front vehicle to the front of the following vehicle. It can be shown that when all the vehicles in the fleet have identical input-output characteristics, i.e. $G_i(s) = G(s)$, then equation (4) holds also for the constant time headway policy with $\overline{G_i}(s) = G(s)$. However, the case when they have different input-output characteristics warrants further investigation.

Case 2: Vehicles with constant time headway policy

Let us consider the case where the vehicles use a constant time headway policy, i.e. the desired intervehicle spacing s_{d_i} is equal to the constant time headway multiplied with the vehicle speed. Let us now consider a string of vehicles that satisfy (1). The position error is given by

$$\delta_i = x_{i-1} - x_i - l_i - h_i \dot{x}_i$$

where h_i is the time headway of the ith vehicle. Using the Laplace or differential operator 's', we have

$$\delta_i = \frac{1}{s}[v_{i-1} - v_i] - l_i - h_i \dot{x}_i$$

For string stability analysis we focus on the upstream propagation of transient position/velocity/acceleration errors characterized by the following equations

$$\delta_i = \frac{1}{s}[(v_{i-1} - v_i) - sh_i v_i] = \frac{1}{s}[1 - G_i - sh_i G_i] v_{i-1}$$

$$v_{ri} = v_{i-1} - v_i = (1-G_i) v_{i-1}$$

$$a_{ri} = \dot{v}_{ri} = \dot{v}_{i-1} - \dot{v}_i$$

or,

$$a_{ri} = s(1-G_i) v_{i-1}$$

which gives us

$$\frac{\delta_i}{\delta_{i-1}} = \frac{1 - G_i - sh_i G_i}{1 - G_{i-1} - sh_{i-1} G_{i-1}} G_{i-1} = \hat{G}_i(s) \tag{5}$$

and

$$\frac{v_{ri}}{v_{ri-1}} = \frac{a_{ri}}{a_{ri-1}} = \frac{(1 - G_i)}{(1 - G_{i-1})} G_{i-1} = \overline{G_i}(s)$$

Theorem 1 (String Stability): The class of interconnected systems of vehicles following each other in a single lane without passing is *string stable* if and only if the impulse response $g_i(t)$ of the error propagation transfer function $G_i(s)$, $\overline{G_i}(s)$ or $\hat{G}_i(s)$, as the case may be, for each individual vehicle in this class satisfies

$$\|g_i\|_1 \leq 1 \qquad \forall \quad i \in N \tag{6}$$

Proof:

If: Assuming $\delta_i, v_{ri}, a_{ri} \in L_p$ and $g_i \in L_1$ where $i \in N$, we have from [7]

$$\begin{aligned} &\|\delta_i\|_p \leq \|g_i\|_1 \|\delta_{i-1}\|_p \\ &\|v_{ri}\|_p \leq \|g_i\|_1 \|v_{ri-1}\|_p \qquad \forall\, p \in [1, \infty] \\ &\|a_{ri}\|_p \leq \|g_i\|_1 \|a_{ri-1}\|_p \end{aligned} \tag{7}$$

Therefore, if we have $\|g_i\|_1 \leq 1 \;\; \forall \;\; i \in N$, then (2) of Definition 2 is satisfied and the system is string stable.

Only If: It can be shown that if condition (6) is not met, i.e. then there exists a position error signal that will lead to string instability for a particular transfer function that does not belong to the *class* of interconnected systems defined in the theorem. For example, if

$$G_i(s) = \frac{s+2}{s^2 + s + 1}$$

we have $g_i(t) = e^{-0.5t} \cos(0.87t) + 1.732 e^{-0.5t} \sin(0.87t)$

and $\|g_i\|_1 > 1$

Consider the error signal

$$\delta_{i-1}(t) = \begin{cases} 1 & 0 \leq t \leq t' \\ 0 & otherwise \end{cases}$$

such that $\|\delta_{i-1}\|_\infty = 1$ and $\delta_{i-1} \in L_p$. We have

$$\delta_i(t) = \int_0^t g_i(t-\tau)\delta_{i-1}(\tau)d\tau = -1.993e^{-0.5t}\cos(0.87t) + 0.004e^{-0.5t}\sin(0.87t) + 1.993\,,\ t < t'$$

$$= \int_0^{t'} g_i(t-\tau)\delta_{i-1}(\tau)d\tau = -1.993e^{-0.5t}\cos(0.87t) + 0.004e^{-0.5t}\sin(0.87t) + 1.993e^{-0.5(t-t')}\cos(0.87(t-t')) - 0.004e^{-0.5(t-t')}\sin(0.87(t-t')),\ t \geq t'$$

Say $t' = 10$, then we get $\|\delta_i\|_\infty \approx 2.4 > \|\delta_{i-1}\|_\infty$ which implies string instability by Definition 4. Similarly it can be also shown that $\|v_{ri}\|_\infty > \|v_{ri-1}\|_\infty$ and $\|a_{ri}\|_\infty > \|a_{ri-1}\|_\infty$ for similar velocity and acceleration error signals.

Remark 2: (i) We should note that the string stability theorem refers to a *class* of systems. For example, the *class* of systems characterized by $\|g_i\|_1 \leq 1 \quad \forall \quad i \in N$ is string stable. The *class* of systems with $\|g_i\|_1 > 1$ for some *i* cannot be guaranteed to be string stable because we can find at least one system in this class that is string unstable. This, however, does not mean that every system with $\|g_i\|_1 > 1$ for some *i* is string unstable. This is due to the fact that the condition $\|g_i\|_1 \leq 1$ is obtained from an inequality that could be conservative.

(ii) In addition to string stability, it is desirable to have $g_i(t) > 0 \quad \forall \quad i \in N \quad \forall t > 0$ in order to avoid oscillatory responses [6].

Lemma 1 (Strict String Stability): The *class* of interconnected systems of vehicles following each other in a single lane without passing is *strictly string stable* if and only if the impulse response $g_i(t)$ of the error propagation transfer function $G_i(s)$, $\overline{G}_i(s)$ or $\hat{G}_i(s)$, as the case may be, for each individual vehicle in this class satisfies

$$\|g_i\|_1 < 1 \qquad \forall \quad i \in N \tag{8}$$

Proof: It is similar to the earlier proof and is omitted.

Remark 3: For the interconnected system of vehicles that we consider in (1), the ICC controllers of the vehicles are designed such that at steady state (zero frequency), the velocity of the following vehicle matches that of the preceding vehicle. This means that we will always have $|G_i(0)| = 1 \quad \forall \quad i \in N$.

It is also desirable to design $G_i(s)$ so that $g_i(t)$ does not change sign in order to avoid oscillatory responses in the error signals that could give rise to undesirable speed fluctuations in traffic flow. If the ICC controllers are designed to guarantee that $g_i(t)$ does not change sign and $|G_i(0)| = 1$, then string stability is guaranteed as stated by the following lemma.

Lemma 2: Assume that $G_i(s)$ is designed so that $g_i(t)$ does not change sign and $|G_i(0)|=1$. Then the system of *N* vehicles with transfer function $G_i(s)$, $i \in N$ is string stable.

Proof:

If the impulse response $g_i(t)$ does not change sign we have

$$||g_i||_1 = \int_0^\infty |g_i(t)|dt = |\int_0^\infty g_i(t)e^{-0t}dt| = |G_i(0)| = 1 \qquad (9)$$

Therefore, condition (2) of Definition 2 is satisfied and the string of vehicles is string stable.

✧

Remark 4: A less conservative bound could be obtained in (7) when p=2. In this case we have [7]

$$\begin{aligned} ||\delta_i||_2 &\le ||G_i(s)||_\infty \, ||\delta_{i-1}||_2 \\ ||v_{ri}||_2 &\le ||G_i(s)||_\infty \, ||v_{ri-1}||_2 \\ ||a_{ri}||_2 &\le ||G_i(s)||_\infty \, ||a_{ri-1}||_2 \end{aligned} \qquad (10)$$

where

$$||G(s)||_\infty = \sup_\omega |G(j\omega)|$$

and from [7]

$$||G_i(s)||_\infty \le ||g_i||_1 \qquad (11)$$

Remark 5: Since $v_i = G_i(s)v_{i-1}$, it follows that for speed following matching at steady state we should have $|G_i(0)|=1$ which means that $||G_i(s)||_\infty \ge 1$. This in turn means that the best we can do in (10) is to design $G_i(s)$ so that $||G_i(s)||_\infty = 1$. Another approach is to design $G_i(s)$ so that $|G_i(0)|=1$ and $|G_i(j\omega)|<1 \quad \forall \omega > 0$. In this case we will have strict string stability ($||\delta_i||_2 < ||\delta_{i-1}||_2$, $||v_{ri}||_2 < ||v_{ri-1}||_2$, $||a_{ri}||_2 < ||a_{ri-1}||_2$) for frequencies $|\omega| > 0$. This approach has already been used in [1,6].

Remark 6: It should be noted that our definition for string stability is conservative. In other words if (2) is violated for some *i*, that does not mean that the response of the string of vehicles is not acceptable. The mixing of vehicles with $G_i(s)$ that satisfies for some *i* and violates for some other *i* the conditions of the string stability theorem (6) will be analyzed in Section 5.

3 String Stability of Manual Traffic

We investigate the string stability of a fleet of manual vehicles closely following each other in a single lane using a human driver car following model from literature. The model is applicable only under conditions of fairly dense traffic in which the driver generally attempts to match his velocity to the car ahead while maintaining some vehicle spacing. The string stability theorem is used to examine whether the model belongs to the class of systems that guarantee string stability. We assume that all vehicles in the fleet have identical input/output characteristics and so by Remark 1 we have the following:

$$\frac{\delta_i}{\delta_{i-1}} = \frac{v_{ri}}{v_{ri-1}} = \frac{a_{ri}}{a_{ri-1}} = \frac{v_i}{v_{i-1}} = G_i(s) = G(s)$$

Thus, to investigate whether the following models belong to the class of systems that guarantee string stability, we analyze the transfer function of each model that relates the velocity of the lead vehicle to that of the following vehicle.

3.1 Pipes Model

This is a linear follow-the-leader model based on car following theory that pertains to single lane dense traffic with no passing and assumes that each driver reacts to a stimulus from the vehicle ahead. The stimulus is the velocity difference and the driver responds with an acceleration command, i.e.

$$Response(t) = Sensitivity \times Stimulus(t - \tau)$$

where τ is the reaction time of the driver-vehicle system.

It can be mathematically expressed as

$$a_f = \frac{\lambda}{M}[v_l(t-\tau) - v_f(t-\tau)] \tag{12}$$

where v_l and v_f are the lead and following vehicle's velocities, respectively, a_f is the following vehicle's acceleration, M is the mass of the following vehicle and λ is a sensitivity factor. The dynamics of the vehicle are modeled by an integrator and the driver's central processing and neuromuscular dynamics by a constant. This model was first proposed by Pipes [8] and later validated by Chandler [9].

The transfer function of the Pipes model is given by

$$G_p(s) = \frac{v_i}{v_{i-1}} = \frac{0.37e^{-1.5s}}{s + 0.37e^{-1.5s}} \tag{13}$$

Evaluating the impulse response we get $||g_p||_1 = 1.1$, implying that the Pipes model does not belong to the class of systems mentioned in the theorem (given by (6)) that guarantee string stability. However, we cannot confirm the existence of slinky effect. Also $g_p(t)$ changes sign for $t>0$ (Fig. 2), which means that the model has an oscillatory response. We also find that $|G_p(j\omega)|>1$ for very small frequencies. As we demonstrate later using simulations, a string of vehicles represented by the Pipes model exhibits string instability. Furthermore, a comparison of the responses of the Pipes model with experiments presented in Section 6 shows that the Pipes model gives a response that is less oscillatory with smaller slinky-type effects than in actual vehicles. Consequently in actual driving one would expect more pronounced slinky-type effects than those predicted by the Pipes model. One reason for this discrepancy is that the human driver models were developed and validated for relatively smooth vehicle following. Among the several human driving models considered the response of the Pipes model was found to be the closest to the one observed during experiments in the presence of transients.

4 String Stability of ICC Vehicular Traffic

Let us now consider the string stability of a fleet of ICC vehicles closely following each other in a single lane. The ICC model given in [1] is used to represent the ICC vehicles. For longitudinal control, the automatic control system of the ICC vehicle may be considered as having two input variables: throttle angle command and brake command, and one output variable: vehicle speed [1]. The other inputs such as aerodynamic drag, road conditions and vehicle mass changes are treated as disturbances. The ICC vehicle is assumed to use a constant time headway policy. We consider the throttle and the brake subsystems separately, as they are not allowed to act simultaneously.

4.1 Throttle Controller

The closed loop transfer function for the throttle subsystem is given by [1]

$$G_{th}(s) = \frac{\delta_i}{\delta_{i-1}} = \frac{(a+bk_1)s^2 + b(k_2+k_3)s + bk_4}{s^3 + (a+bk_1+bk_2h)s^2 + b(k_2+k_3+k_4h)s + bk_4} \qquad (14)$$

where k_1, k_2, k_3, k_4: are the controller parameters to be designed; h is the desired time headway and a, b: are constants that depend on the operating point which is the speed of the vehicle ahead

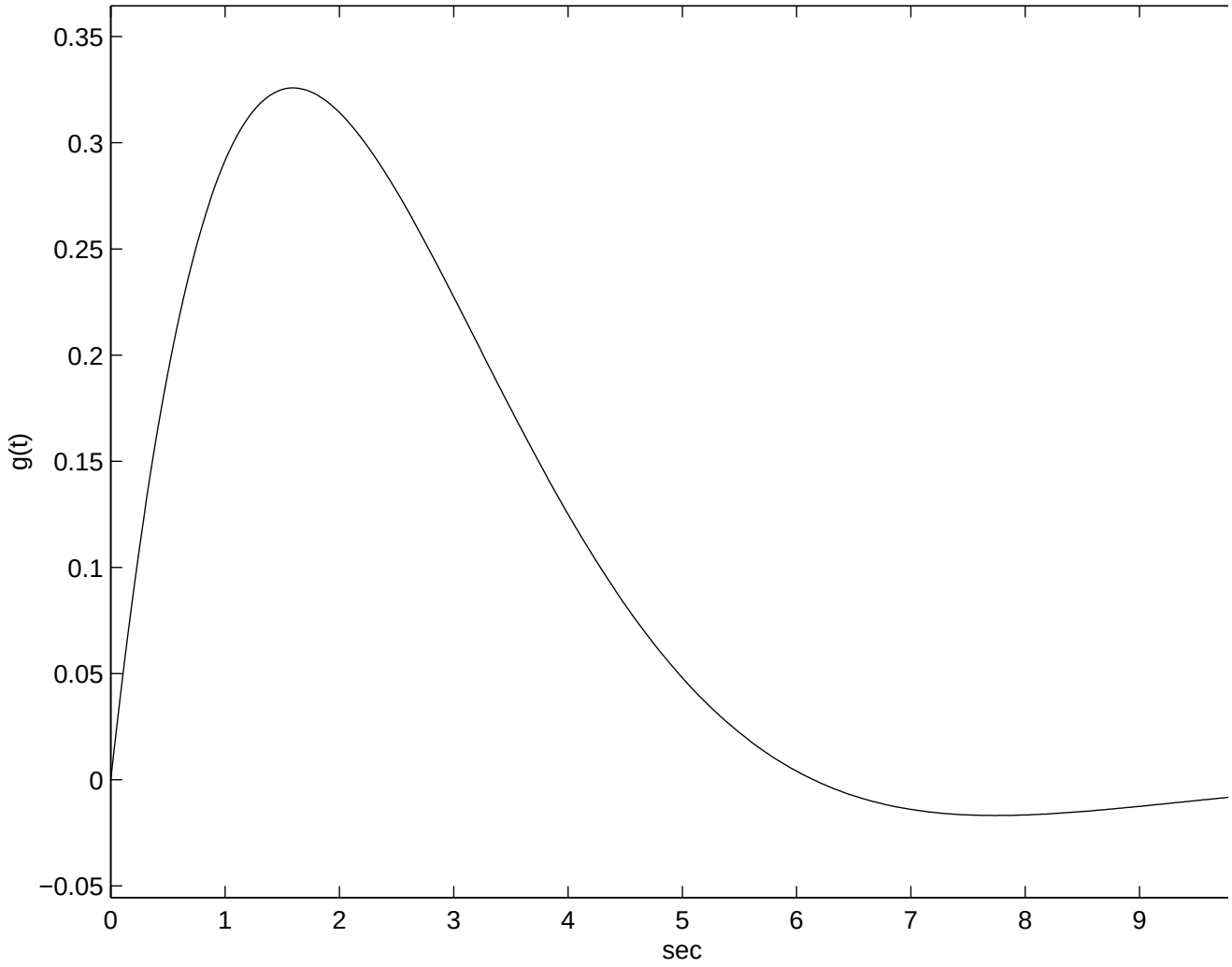

Figure 2(a): Pipes linear car following model: Impulse response $g_p(t)$ vs. *t.*

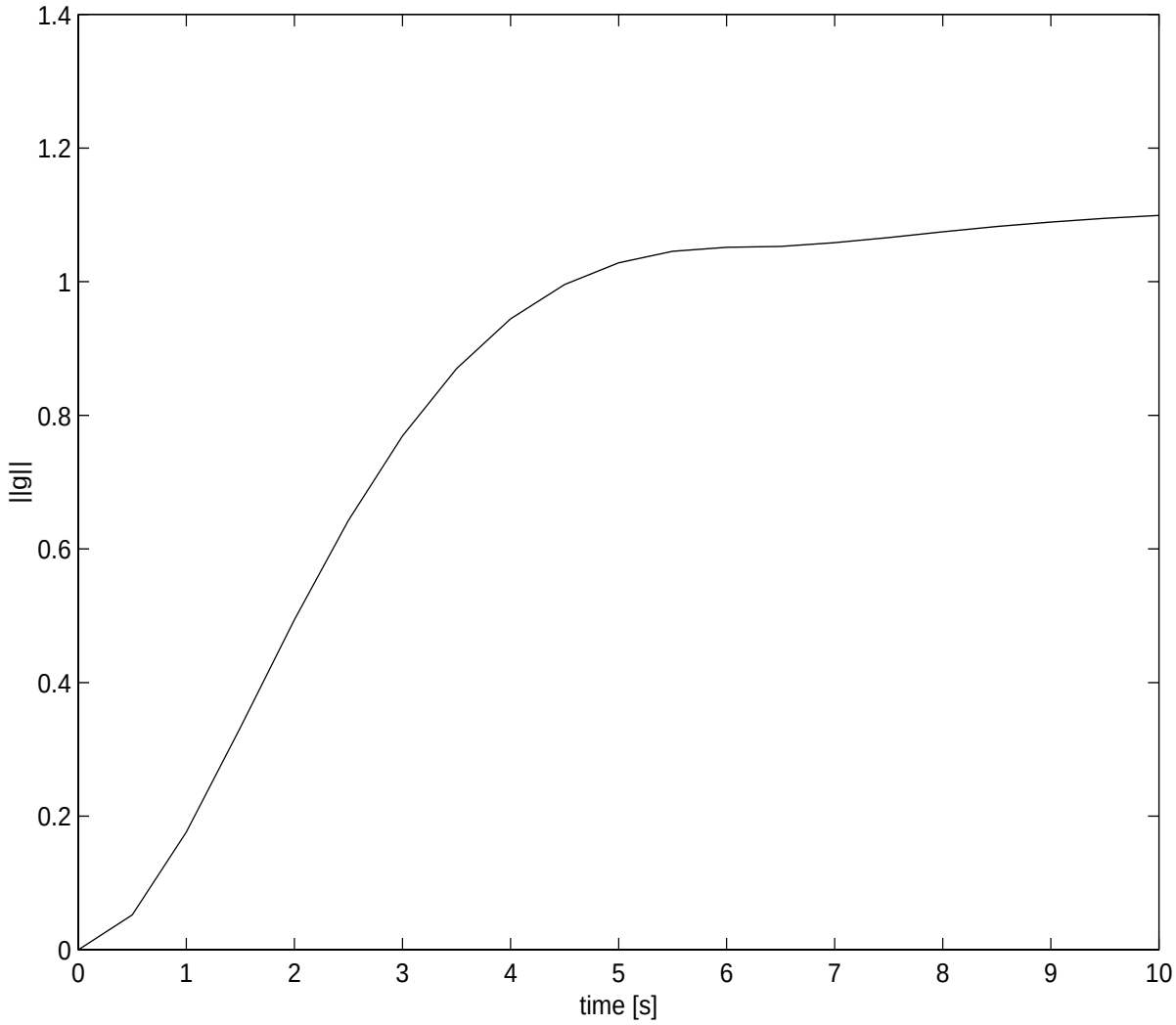

Figure 2(b): Pipes linear car following model: $\int_0^t |g_p(\tau)| d\tau$ vs. t.

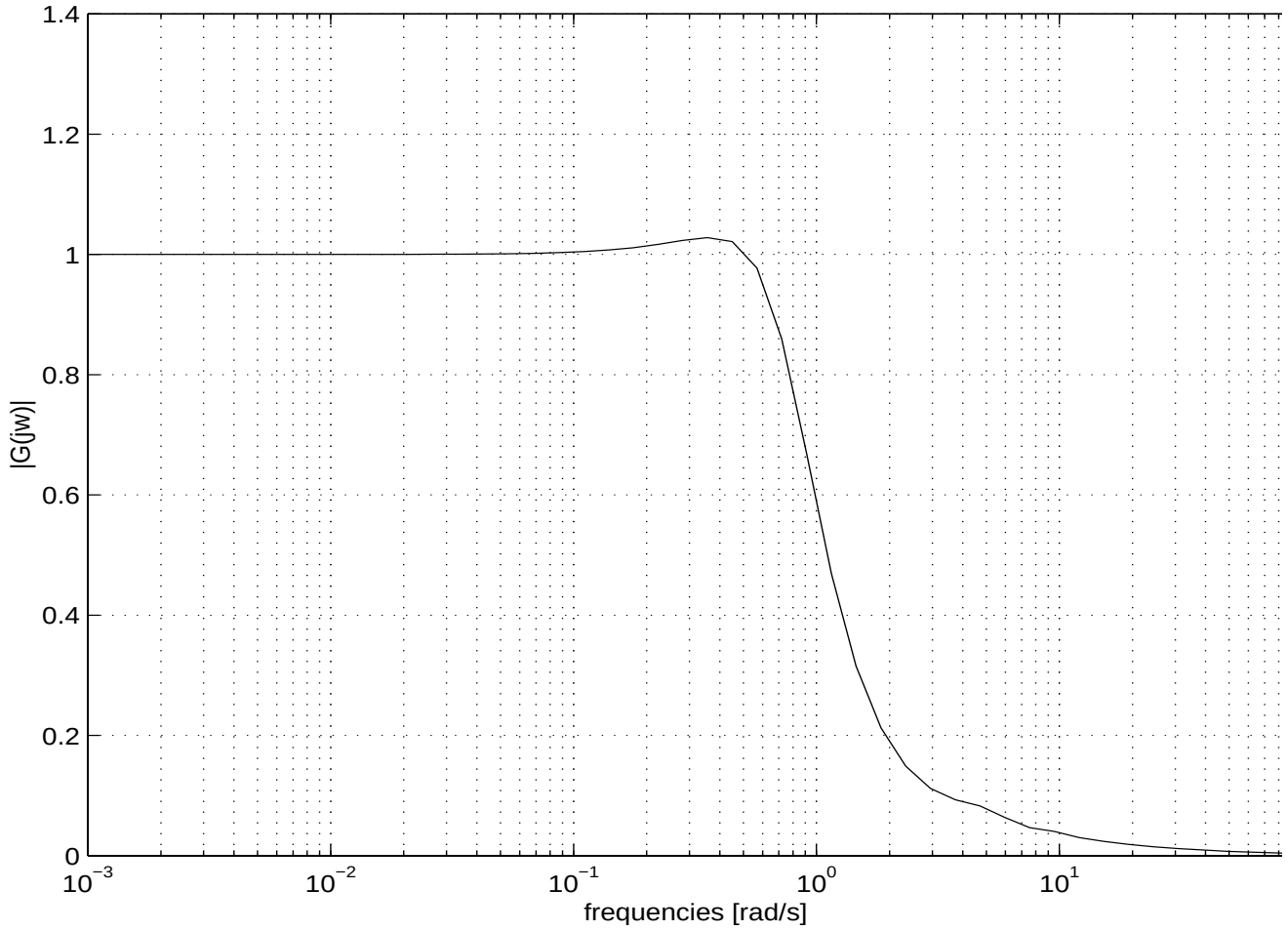

Figure 2(c): Pipes linear car following model:$|G_p(j\omega)|$ vs. ω.

The throttle controller is designed to control the throttle angle of the ICC vehicle using the design controller parameters k_1 to k_4 that are chosen using pole placement as follows [1]:

$$\begin{aligned} k_1 &= (\lambda_0 + 2\zeta\omega_n - bk_2h - a)/b \\ k_2 &= 0.2/b \\ k_3 &= (2\zeta\omega_n\lambda_0 + \omega_n^2 - bk_2 - h\lambda_0\omega_n^2)/b \\ k_4 &= \lambda_0\omega_n^2/b \end{aligned} \tag{15}$$

where λ_0 is a desired pole;ω_n, ζ is the natural frequency and damping ratio of the two desired complex poles, respectively.

The throttle controller in (14) is applied to a validated nonlinear vehicle model and tested through a series of simulations with the following parameter values that satisfy the performance criteria [1]

$\lambda_0 = 1.2$, $\omega_n = 0.1$, $\zeta = 1$ and a constant time headway h=1 sec.

Using these values in (15) to get the controller parameter values and substituting them in (14) we obtain

$$G_{th}(s) = \frac{1.2s^2 + 0.24s + 0.012}{s^3 + 1.4s^2 + 0.25s + 0.012} \tag{16}$$

The L_1 norm of the throttle subsystem (16) is

$$\|g_{th}\|_1 = 1$$

Also the impulse response $g_{th}(t) > 0$ for all t>0 (Fig. 3). Thus, the throttle controller of the ICC vehicle belongs to the class of systems that guarantee string stability. Moreover, $|G_{th}(j\omega)|$ is less than unity for all $\omega > 0$.

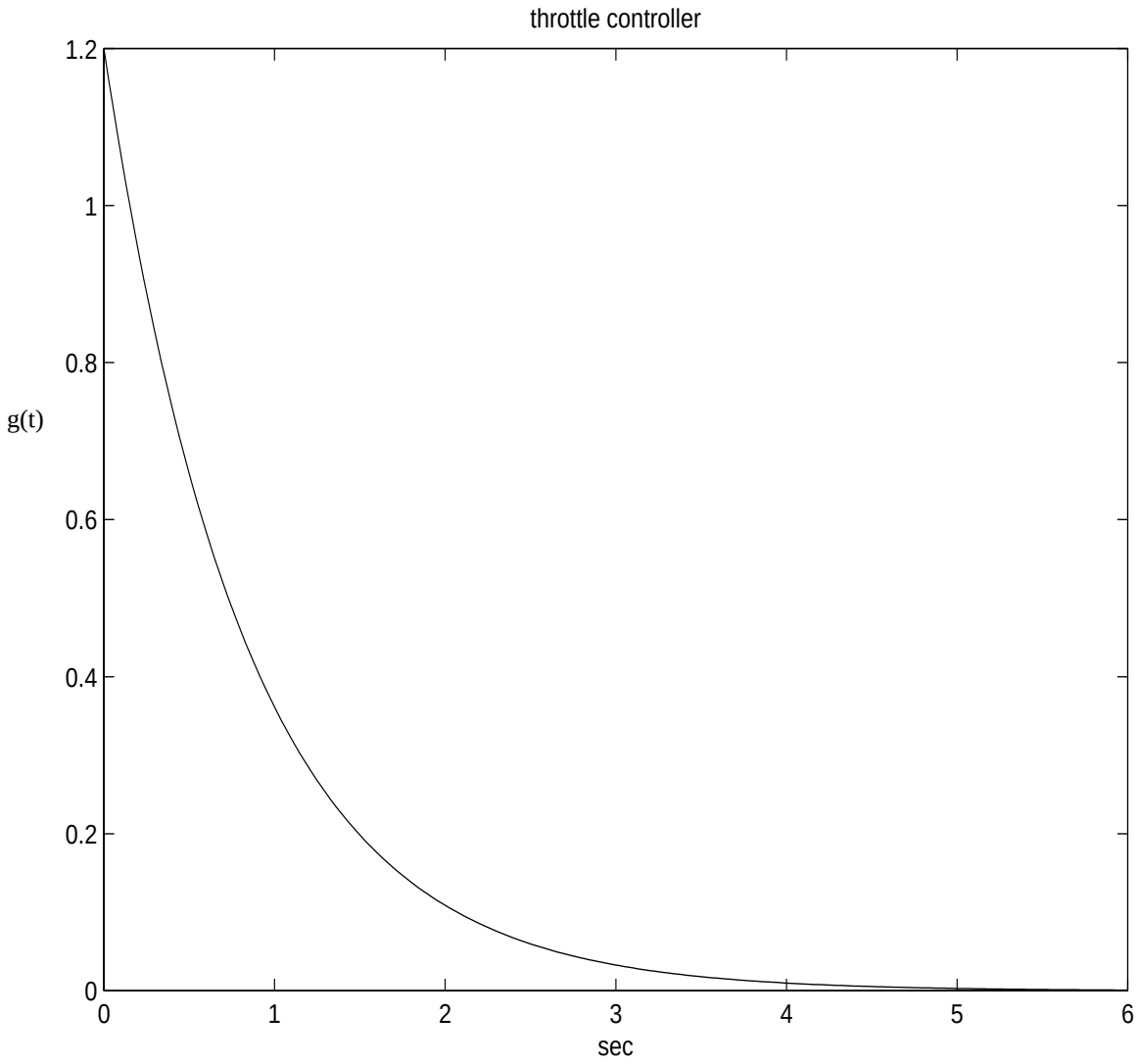

Figure 3(a): Throttle controller subsystem: Impulse response $g_{th}(t)$ vs. t.

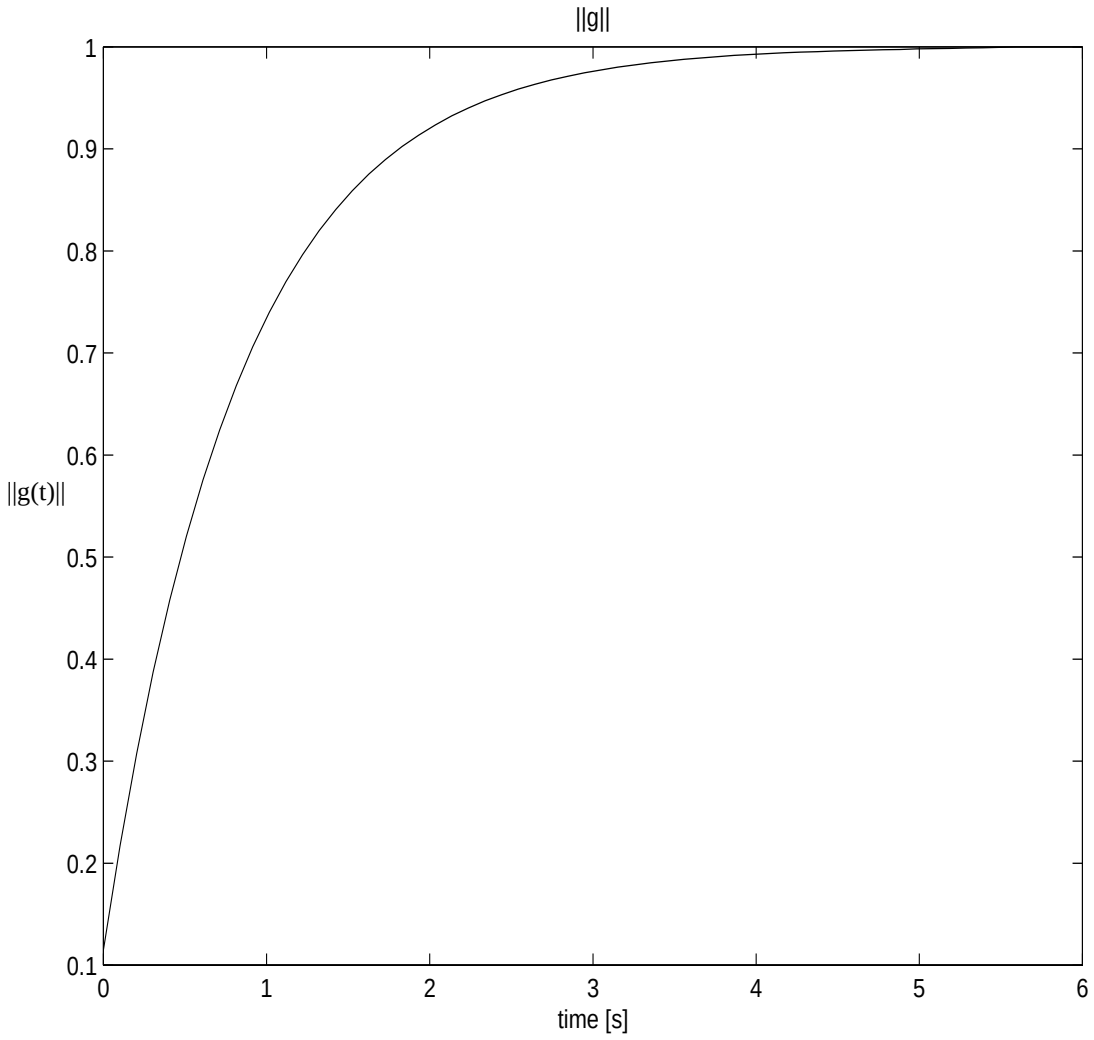

Figure 3(b): Throttle controller subsystem: $\int_0^t |g_{th}(\tau)| d\tau$ vs. t.

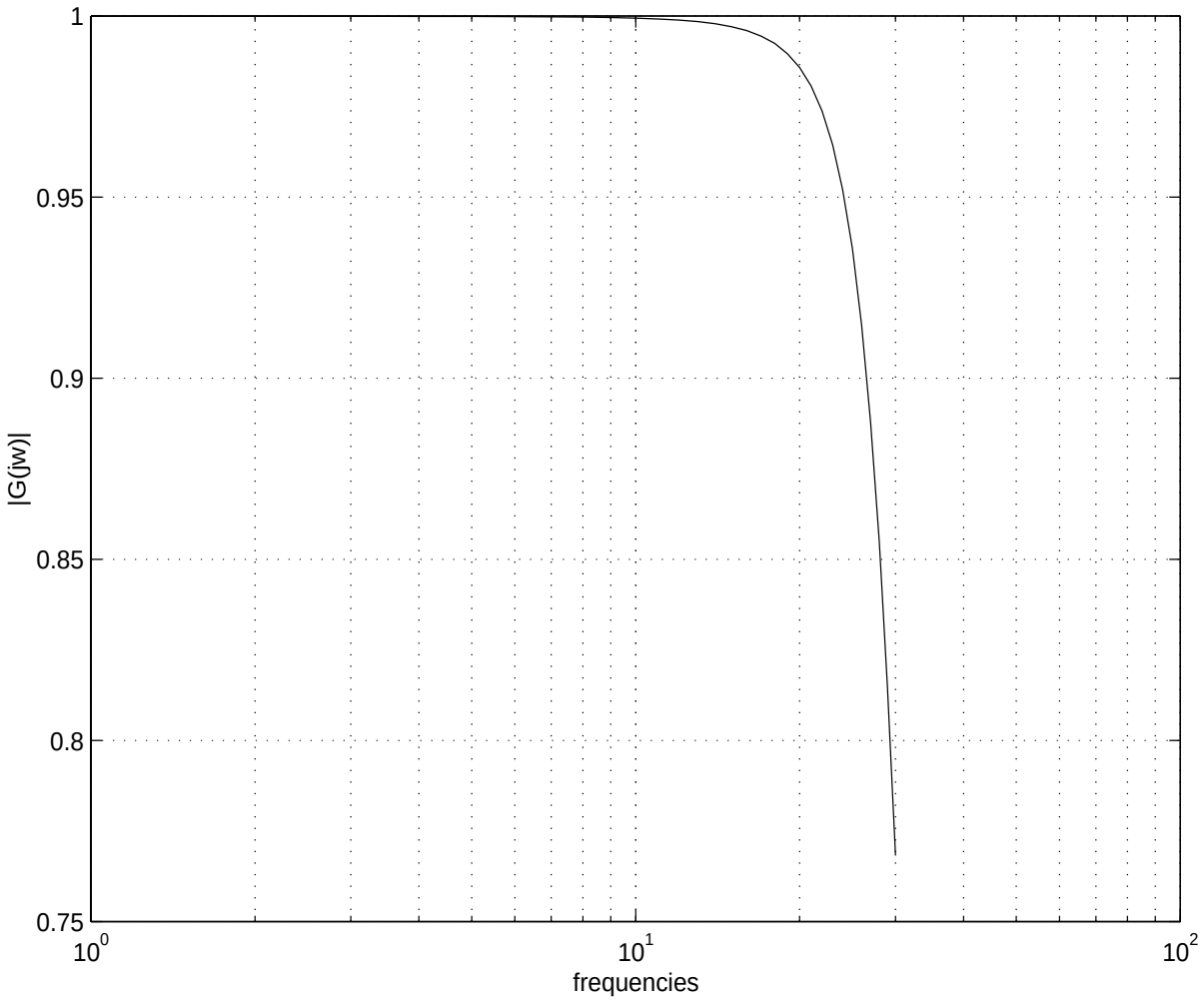

Figure 3(c) Throttle controller subsystem: $|G_{th}(j\omega)|$ vs. ω.

Human factors considerations dictate that the response of an ICC vehicle should be smooth. Therefore, there are two constraints imposed on the throttle controller due to smooth ride requirements [1]. The constraints are the following:

C-I: $a_{\min} \le \dot{V}_f \le a_{\max}$ where $a_{\min}$ and $a_{\max}$ are specified.

C-II: The absolute value of the jerk defined as $\ddot{V}_f$ should be as small as possible.

The controller in (16) does not guarantee that the above two constraints will always be satisfied. For example, if the lead vehicle rapidly changes its velocity at a particular point, it may create a large relative velocity error and spacing error, which in turn may cause large, throttle angle and acceleration, violating C-I and C-II. Also there may be large initial position and velocity errors when the following vehicle switches from one leading vehicle to another due to lane change, merging etc., leading to high

acceleration/deceleration that may violate C-I, C-II. In order to avoid these occurrences, two limiters are used in the throttle controller of [1].

The first is an acceleration limiter to protect the ICC vehicle from responding to erratic behavior of the leading vehicle. The velocity of the leading vehicle V_l is passed through an acceleration limiter shown in Fig. 4 where p is some positive constant. Instead of following V_l the throttle controller is designed to follow $\hat{V}_l$. The acceleration limiter limits the maximum and minimum acceleration of the target velocity to $a_{\max}$ and $a_{\min}$, respectively. It eliminates any sudden changes in V_l during transients and presents a smooth target velocity for the controller to follow. At steady state, $\hat{V}_l$ approaches V_l, therefore following the former the throttle controller will eventually reach V_l in a smooth way.

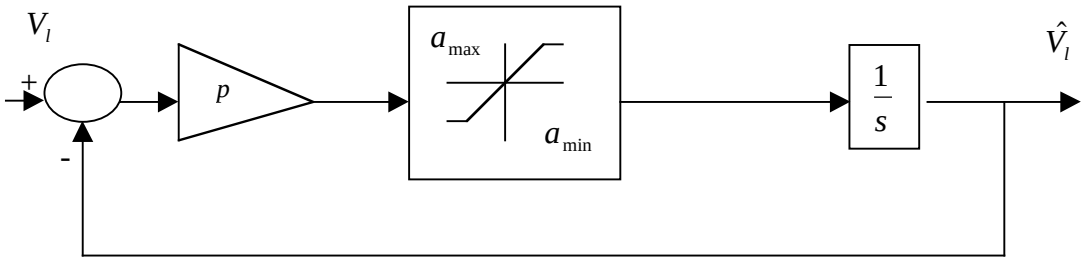

Figure 4: Acceleration Limiter.

In 100% ICC vehicular traffic, the acceleration limiter will not affect string stability since all vehicles (with the exception of emergency stopping) are assumed to operate within the limits of $a_{\max}$ and $a_{\min}$. In mixed traffic this may not be the case because the manually driven vehicles may generate trajectories outside the desired acceleration limits.

In addition to the acceleration limiter, the spacing error is passed through a saturation element to take care of large spacing errors being fed into the controller. The saturation element $sat(\delta)$ is defined as

$$sat(\delta) = \begin{cases} e_{\max} & if \quad \delta > e_{\max} \\ e_{\min} & if \quad \delta < e_{\min} \\ \delta & otherwise \end{cases}$$

This prevents any large spacing error and limits the spacing error measurements seen by the throttle controller to be within $e_{\max}$ and $e_{\min}$. In other ICC designs similar modifications are used to maintain smooth response.

4.2 Brake Controller

For the closed loop brake subsystem we have the following transfer function [1]

$$G_{br}(s) = \frac{v_i}{v_{i-1}} = \frac{k_5 s + k_6}{s^2 + (k_5 + k_6 h)s + k_6} \tag{17}$$

where k_5, k_6: brake controller gains
h: time headway desired

Equation (17) is investigated for $h = 1s$ with the following gains that satisfy the performance criteria given in [1]

$$k_5 = 1$$
$$k_6 = 0.25$$

From the impulse response of (17) we have

$$||g_{br}||_1 = 1$$

and $g_{br}(t) > 0$ for all $t > 0$ (Fig. 5) implying that the brake controller does not have an oscillatory response. Hence, like the throttle controller, the brake controller also belongs to the class of systems that guarantee string stability. Furthermore, $|G_{br}(j\omega)|$ is less than unity for all $\omega > 0$.

Therefore, we have shown that both the throttle and the brake subsystems belong to the class of systems that guarantee string stability provided that they remain within the saturation limits used. It is important to note that the design parameters of the controllers can be modified such that the throttle and the brake controller subsystems violate (6) and not belong to the class of systems that guarantee string stability.

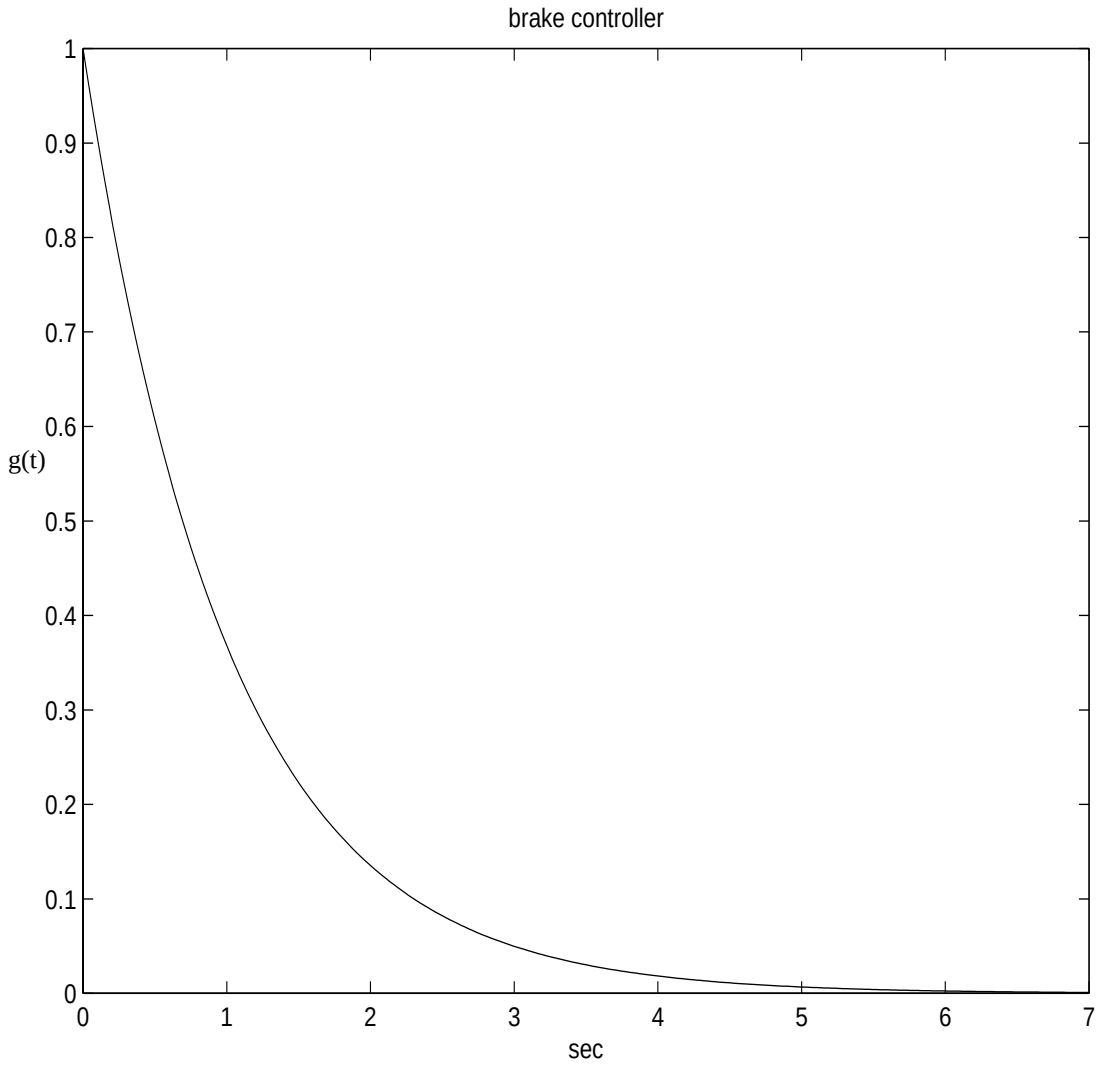

Figure 5(a): Brake controller subsystem: Impulse response $g_{br}(t)$ vs. t.

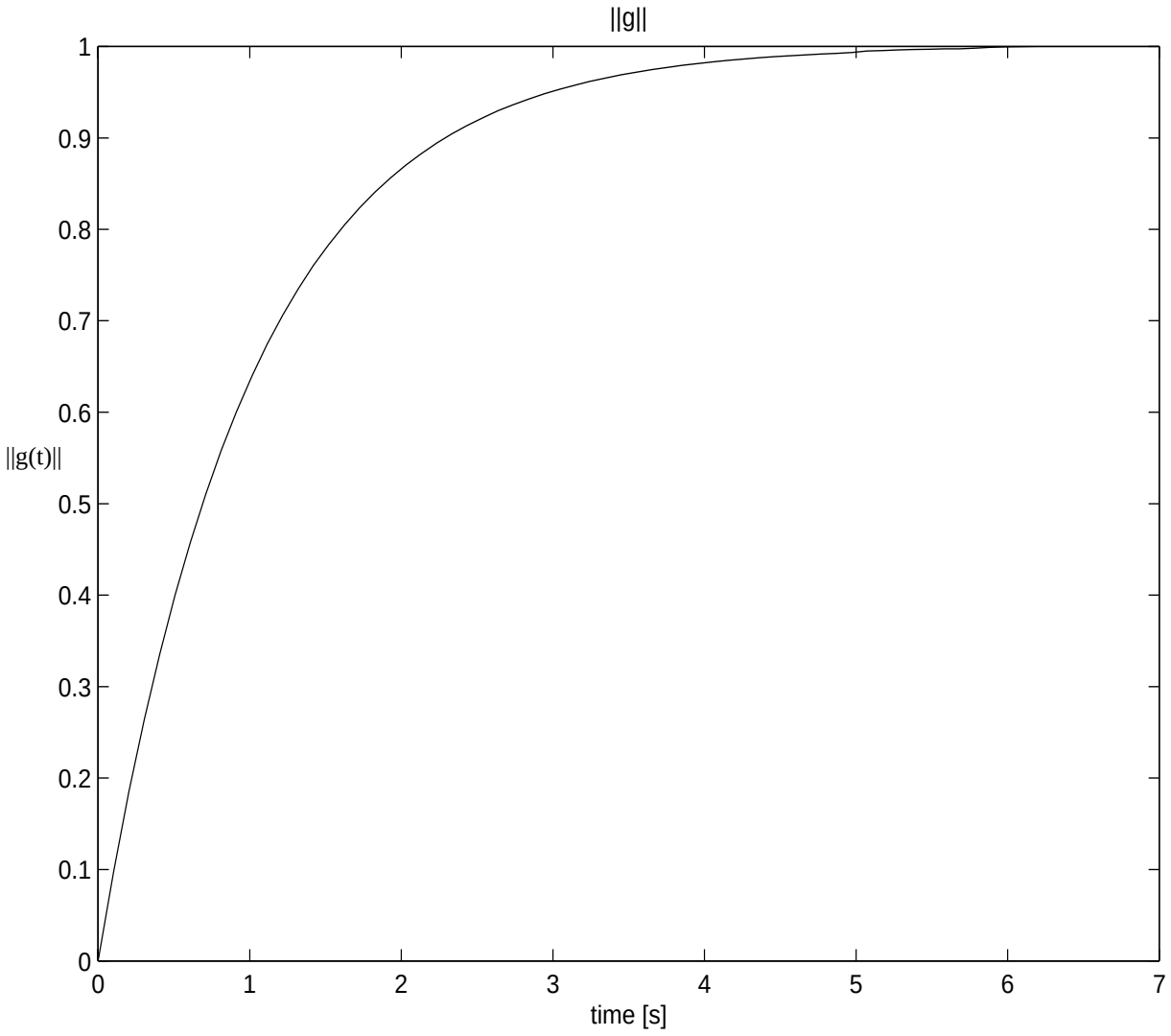

Figure 5(b): Brake controller subsystem: $\int_0^t |g_{br}(\tau)| d\tau$ vs. t.

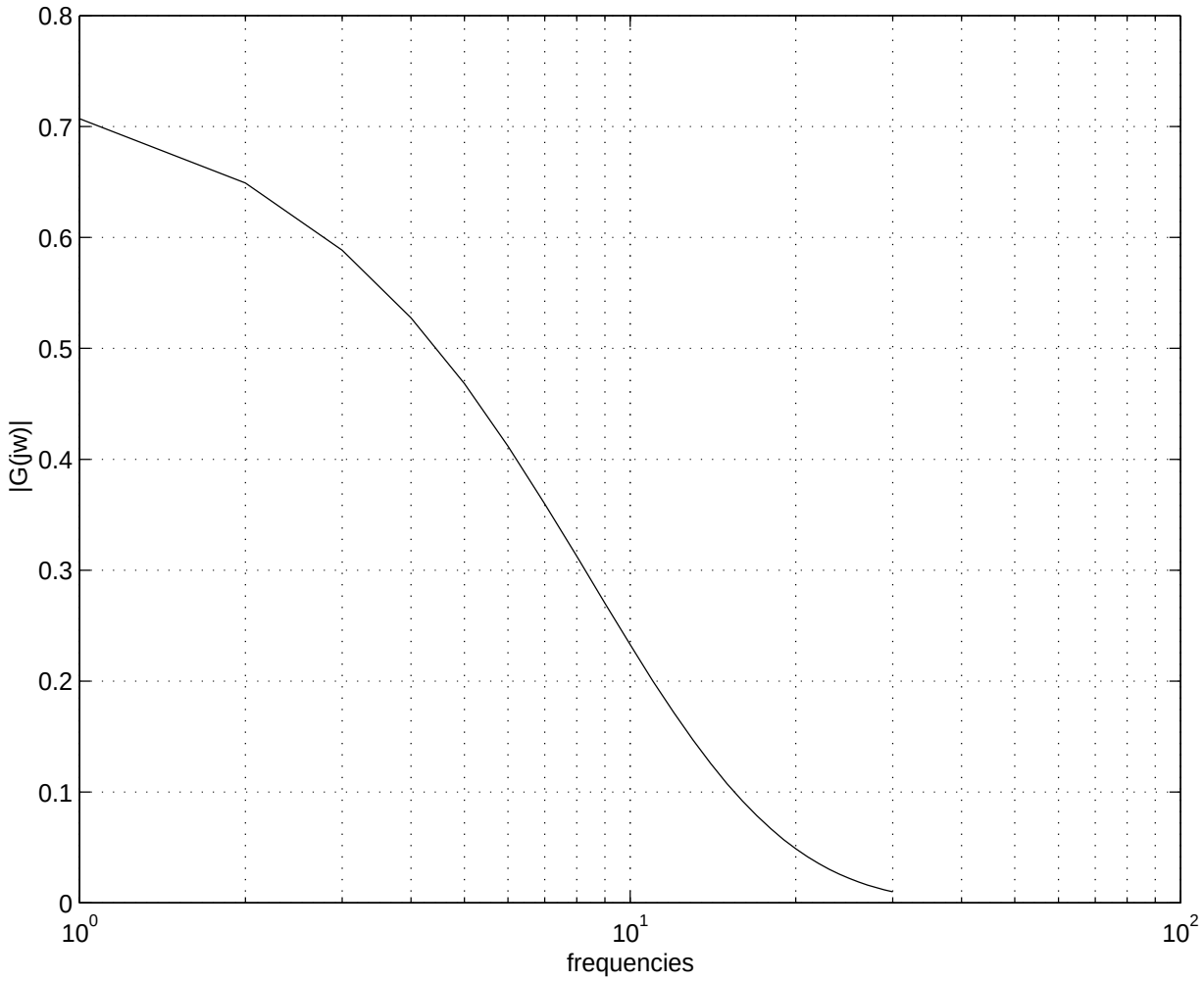

Figure 5(c): Brake controller subsystem: $|G_{br}(j\omega)|$ vs. ω.

5 String Stability of Mixed Vehicles

The mixed traffic system consists of manual and ICC vehicles whose dynamics are given by the models presented in the previous Sections. Consider the manual vehicles to be represented by the Pipes model, which does not belong to the class of systems that guarantee string stability and may generate slinky-type effects. Therefore, we cannot guarantee string stability for the system of mixed vehicles.

However, as stated before, Definition 2 of string stability is conservative. Though the string of mixed vehicles may not be string stable, the behavior of the whole system may be acceptable. We carry out an analysis that should provide some insight into the dynamics of mixed traffic during transients. Consider vehicle following transients for two different cases:

(i) Lead manual vehicle in mixed traffic performs a smooth acceleration maneuver.

(ii) Lead manual vehicle in mixed traffic performs a rapid acceleration maneuver.

5.1 Lead manual vehicle in mixed traffic performs a smooth acceleration maneuver

Using the ICC model presented in the previous Section to represent ICC vehicles, a smooth acceleration maneuver by a lead manual vehicle means that the target speed is within the saturation limits of the ICC acceleration limiter. Considering mixing of vehicles of different classes, we get the error propagation transfer functions as (from (4) and (5))

$$\frac{\delta_i}{\delta_{i-1}} = \frac{1 - G_i - sh_iG_i}{1 - G_{i-1} - sh_{i-1}G_{i-1}} G_{i-1} = G_{ii-1}(s) \tag{18}$$

$$\frac{v_{ri}}{v_{ri-1}} = \frac{a_{ri}}{a_{ri-1}} = \frac{(1-G_i)}{(1-G_{i-1})} G_{i-1} = \overline{G_i}(s) \tag{19}$$

Examining (18) we can conclude that given $G_i(s)$ there may exist an h_i э $1 - G_i(s) - sh_iG_i(s) = 0 \ \forall s$. The existence of such h_i is given by the following lemma.

Lemma 3: A constant h_i exists for a given $G_i(s) = \frac{n(s)}{d(s)}$ such that $1 - G_i(s) - sh_iG_i(s) = 0 \quad \forall s$ if and only if degree ($d(s)$)-degree ($n(s)$)=1 and for $d(s) = s^n + a_1s^{n-1} + \ldots\ldots + a_{n-1}s + a_n$ and $n(s) = b_1s^{n-1} + b_2s^{n-2} + \ldots\ldots + b_{n-1}s + b_n$, where a_1, $a_2, \ldots, a_n$, b_1, $b_2, \ldots, b_n$ are constants with $a_n = b_n$, the following is true

$$\frac{b_{n-1}}{a_{n-1}b_1 - b_n} = \ldots\ldots = \frac{b_1}{a_1b_1 - b_2} = \frac{1}{b_1} = h > 0 \tag{20}$$

where $h_i = h$.

The proof is simple and is omitted.

✧

The existence of h_i to satisfy Lemma 3 exactly is a singular case. The use of h_i however, guarantees that the following vehicle will maintain zero position, velocity and acceleration errors during vehicle following. In other words, with h_i the two vehicles, lead and following will be electronically connected and behave as a single vehicle. Choosing h_i to satisfy Lemma 3 is not practical. However, choosing a time headway close to h_i is possible leading to tight vehicle following. This is demonstrated in the following example:

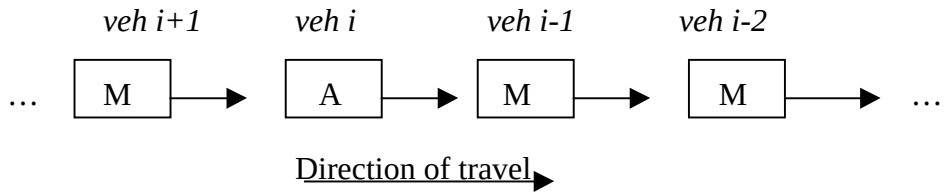

A: ICC vehicle
M: manual vehicle

Figure 6: Mixed manual/ICC traffic.

Consider a string of mixed manual/ICC vehicles as depicted in Fig. 6. Vehicle *i* is an ICC vehicle while vehicle *i-1* and the rest are manual vehicles. All vehicles are assumed to follow a constant time headway policy.

We choose Pipes model [8,9] to represent manually driven vehicles since we demonstrate that it models the slinky-type effects we observe in today's traffic (Section 6). We assume that the ICC vehicles follow a time headway of 1.0s. For manual vehicles, it is difficult to assume a fixed number since different drivers have different driving characteristics. However, for our analysis we assume that the manual vehicles follow a time headway of 1.8s, which is taken as the "national average" for manual traffic [16]. Later we analyze different time headway scenarios. Therefore, we have

$$\frac{\delta_i}{\delta_{i-1}} = \frac{1 - G_{th} - sG_{th}}{1 - G_p - 1.8sG_p} G_p = G_{ii-1}(s) \tag{21}$$

where $G_p(s)$ is taken from (13) and $G_{th}(s)$ is the transfer function of the throttle controller of the ICC vehicle. The time delay is approximated using

$$e^{-Ts} \approx \frac{1}{1+Ts}$$

to obtain

$$G_p(s) = \frac{0.37}{1.5s^2 + s + 0.37}$$

and from (16)

$$G_{th}(s) = \frac{1.2s^2 + 0.24s + 0.012}{s^3 + 1.4s^2 + 0.25s + 0.012}$$

So after substituting for $G_p(s)$ and $G_{th}(s)$ in (21) and rearranging the terms, we have

$$\frac{\delta_i}{\delta_{i-1}} = -\frac{0.074s^3 + 0.014s^2 + .0007s}{1.5s^5 + 2.434s^4 + 0.8426s^3 + 0.1015s^2 + 0.004s} = G_{ii-1}(s)$$

The gain of the velocity and the acceleration errors is given by (19)

$$\frac{v_{ri}}{v_{ri-1}} = \frac{a_{ri}}{a_{ri-1}} = \frac{(1-G_i)}{(1-G_{i-1})} G_{i-1} = \overline{G_i}(s)$$

where

$$\overline{G_i} = \frac{(1-G_{th})}{(1-G_p)} G_p = \frac{0.37s^3 + 0.074s^2 + .0037s}{1.5s^5 + 3.1s^4 + 1.775s^3 + 0.268s^2 + 0.012s} = \tilde{G}_{ii-1}(s)$$

Calculating the impulse responses of the above two error systems, we get

$$g_{ii-1}(t) = 0.051e^{-1.12t} - 0.05e^{-0.222t} - 0.016e^{-0.107t} + 0.014e^{-0.094t}$$

and

$$\tilde{g}_{ii-1}(t) = -0.463e^{-1.2t} + 0.463e^{-0.667t}$$

We find that $||g_{ii-1}||_1 = 0.175$ and $||\tilde{g}_{ii-1}||_1 = 0.308$ which shows that the ICC vehicle attenuates the position, velocity and acceleration errors and does not contribute to the slinky effect phenomenon. On the other hand, if vehicle *i* was a manually driven vehicle in manual vehicle traffic, the error propagation would be given by $||g_p||_1 = 1.1$ as shown in Section 3, from which we could not exclude the possibility of error amplification or the existence of slinky-type effects.

We can verify from (21) that the impulse response $g_{ii-1}(t)$ of $G_{ii-1}(s)$ depends on the headways of manual and ICC vehicles. It is possible to have manual vehicles follow headways other than the mean value of 1.8s. Also some ICC vehicles may be programmed to use headways other than 1.0s. To carry out the above analysis under such varied situations, we can use the plots in Fig. 7. The area under the curve of $g_{ii-1}(t)$ is plotted in Fig. 7(a) as a function of the ICC vehicle headway from 0.5s to 1.5s for different manual vehicle headway of 1.0s, 1.8s and 2.2s, and is a linear function of h_i, the ICC vehicle headway. The $||g_{ii-1}||_1$ is plotted in Fig. 7(b) while Fig. 7(c) plots $||g_{ii-1}||_1$ as a function of manual vehicle headway from 0.7s to 2.2s for different ICC vehicle headway of 0.5s, 1.0s and 1.5s. Using Lemma 3 we can show that for *h*=1/1.2 we have $||g_{ii-1}||_1$=0 as seen in Fig. 7(b).

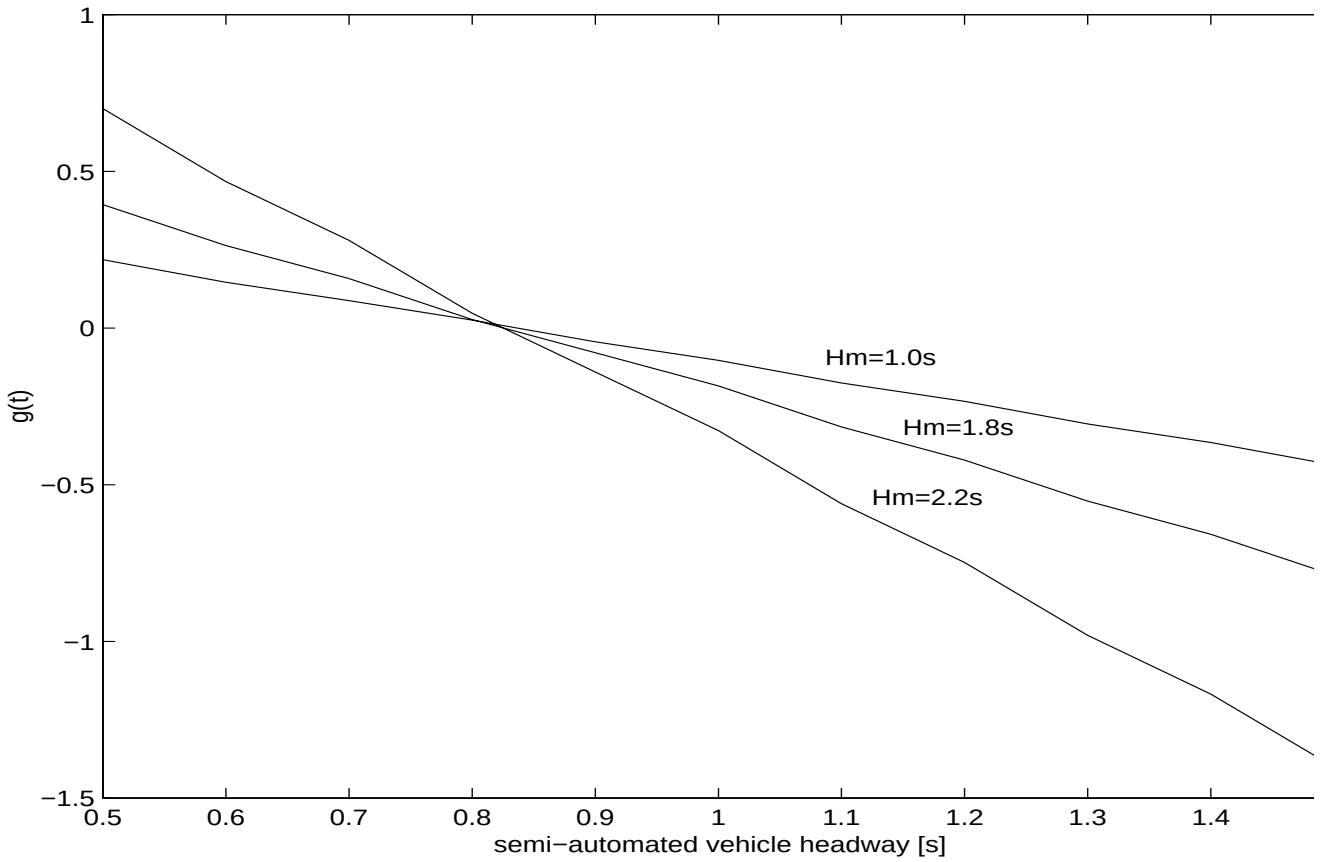

Figure 7(a): Area under the curve of $g_{ii-1}(t)$ as a function of ICC vehicle headway from 0.5s to 1.5s for different manual vehicle headways of 1.0s, 1.8s and 2.2s.

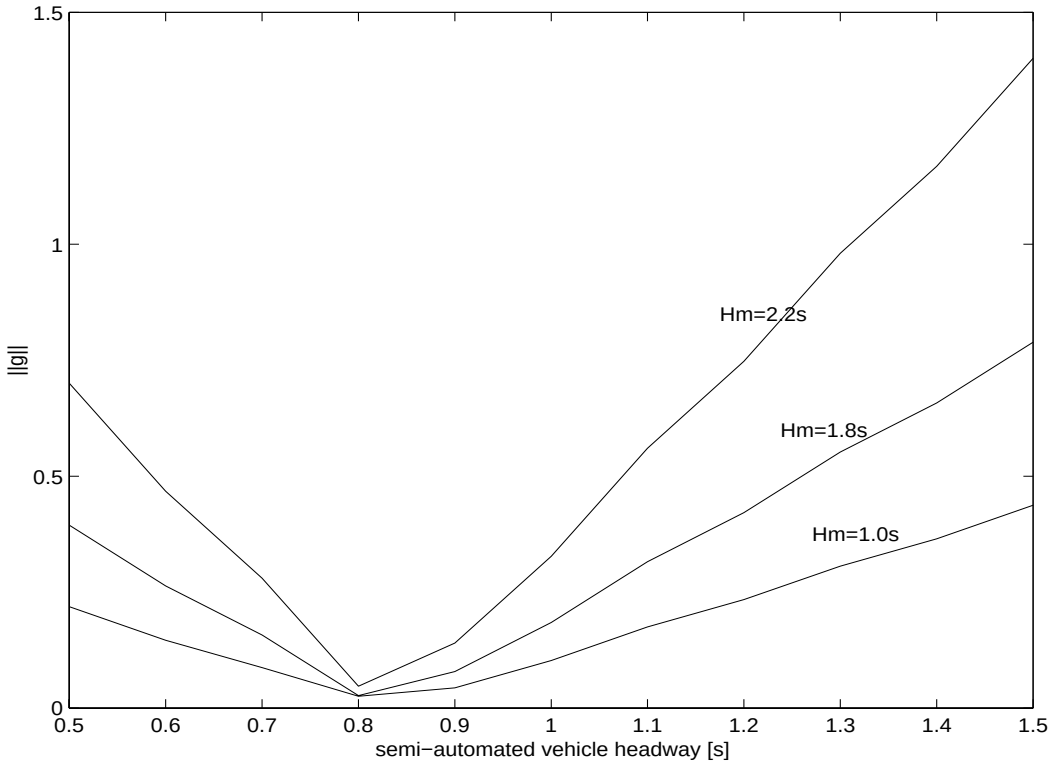

Figure 7(b): $||g_{ii-1}||_1$ as a function of ICC vehicle headway from 0.5s to 1.5s for different manual vehicle headways of 1.0s, 1.8s and 2.2s.

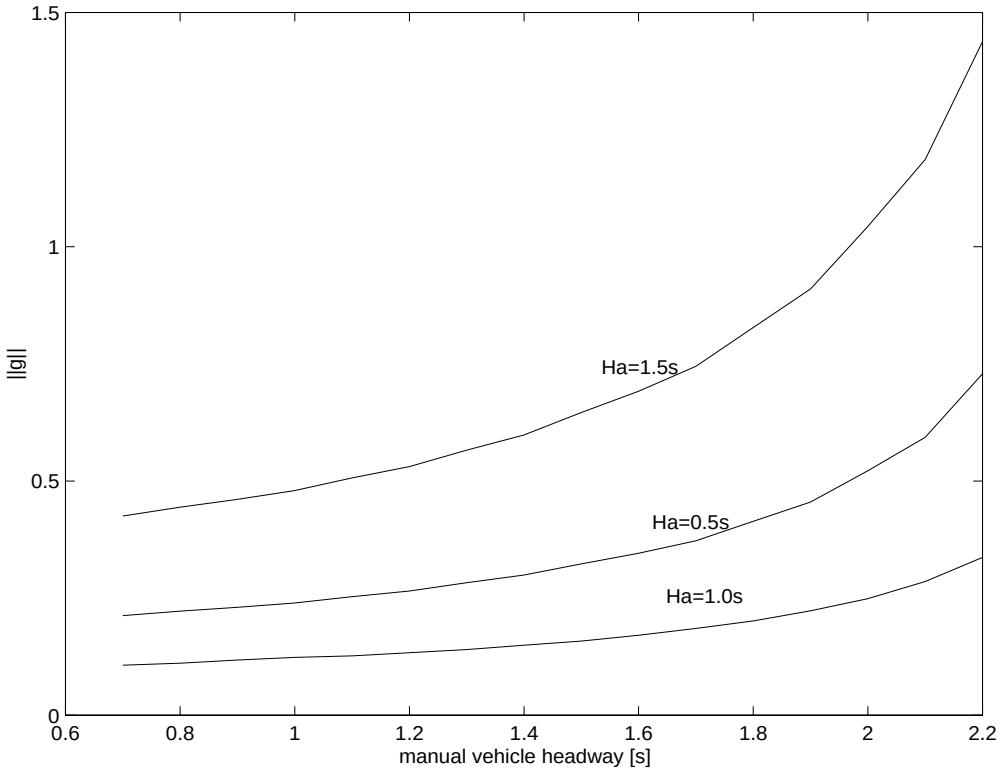

Figure 7(c): $\|g_{ii-1}\|_1$ as a function of manual vehicle headway from 0.6s to 2.2s for different ICC vehicle headways of 0.5s, 1.0s and 1.5s.

To analyze the effect of error attenuation by an ICC vehicle on the following vehicle, let us consider the position, velocity and acceleration errors for manual vehicle *i+1*. We have

$$\frac{\delta_{i+1}}{\delta_i} = \frac{1 - G_p - 1.8sG_p}{1 - G_{th} - sG_{th}} G_{th}$$

$$= -\frac{1.8s^4 + 0.7608s^3 + 0.0982s^2 + 0.004s}{0.3s^5 + 0.26s^4 + 0.117s^3 + 0.0168s^2 + 0.0007s} = G_{ii+1}$$

and

$$\frac{v_{ri+1}}{v_{ri}} = \frac{a_{ri+1}}{a_{ri}} = \frac{(1 - G_p)}{(1 - G_{th})} G_{th}$$

$$= \frac{1.8s^4 + 1.56s^3 + 0.258s^2 + 0.012s}{1.5s^5 + 1.3s^4 + 0.585s^3 + 0.084s^2 + 0.0037s} = \tilde{G}_{ii+1}$$

The impulse responses are given by

$$g_{ii+1}(t) = -5.99e^{-0.333t}\cos(0.369t) + 1.829e^{-0.333t}\sin(0.369t) + 0.041e^{-0.127t} - 0.051e^{-0.074t}$$

$$\tilde{g}_{ii+1}(t) = 1.2e^{-0.333t}\cos(0.368t) + 1.086e^{-0.333t}\sin(0.368t)$$

We obtain $\|g_{ii+1}\|_1 = 11.78$ and $\|\tilde{g}_{ii+1}\|_1 = 3.88$ which shows that the manual vehicle following the ICC vehicle may amplify the position, velocity and acceleration errors. So no conclusion is possible for the tracking errors of vehicle *i+1* from the above analysis.

5.2 Lead manual vehicle in mixed traffic performs a rapid acceleration maneuver

Using the ICC model for ICC vehicles, a rapid acceleration maneuver by the lead manual vehicle means acceleration at a rate greater than $a_{\max}$. In such circumstances we later demonstrate that the ICC vehicle improves traffic flow characteristics. It filters the response of the rapidly accelerating lead manual vehicle in an effort to maintain smooth driving. This is done at the expense of larger position, velocity and acceleration errors and sometimes at the expense of falling far behind the vehicle ahead when the vehicle spacing becomes larger than that stipulated by the constant time headway policy. This smoothing of traffic flow by the ICC vehicle is beneficial for the environment, as we shall observe in Section 7.

6 Simulations and Experiments

6.1 Manual Traffic

We compare the Pipes human driver car following model with the response of an actual manual driver. Experiments were conducted using two manually driven vehicles following each other in a single lane. The lead driver was instructed to speed up from 37mph (~17 m/s) to 45 mph (~20 m/s), slow down to about 30 mph (~14 m/s) and then speed up to 50 mph (~23 m/s). The driver of the following vehicle was instructed to follow the lead vehicle using comfortable time headway. The speed profile generated by the lead vehicle was used as input to the Pipes model in simulation and the response was compared to the response of the actual vehicle. As shown in Fig. 8, the Pipes model gives a smooth approximation of the manual driving response. The experimental vehicle response has greater overshoots and undershoots than the Pipes model. Thus, the results obtained using Pipes model could be viewed as being more conservative than those observed in practice. The experimental comparison results shown in Fig. 8 are found to be similar with several different drivers.

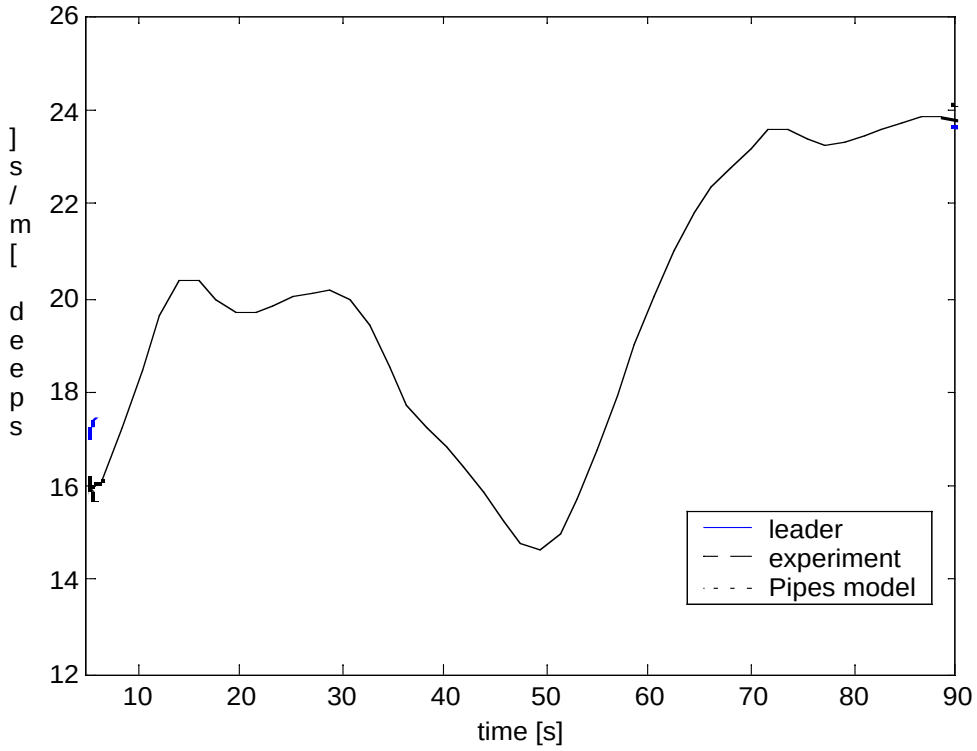

Figure 8: Comparison of response of Pipes model with an actual manual vehicle response in a manual traffic vehicle following scenario.

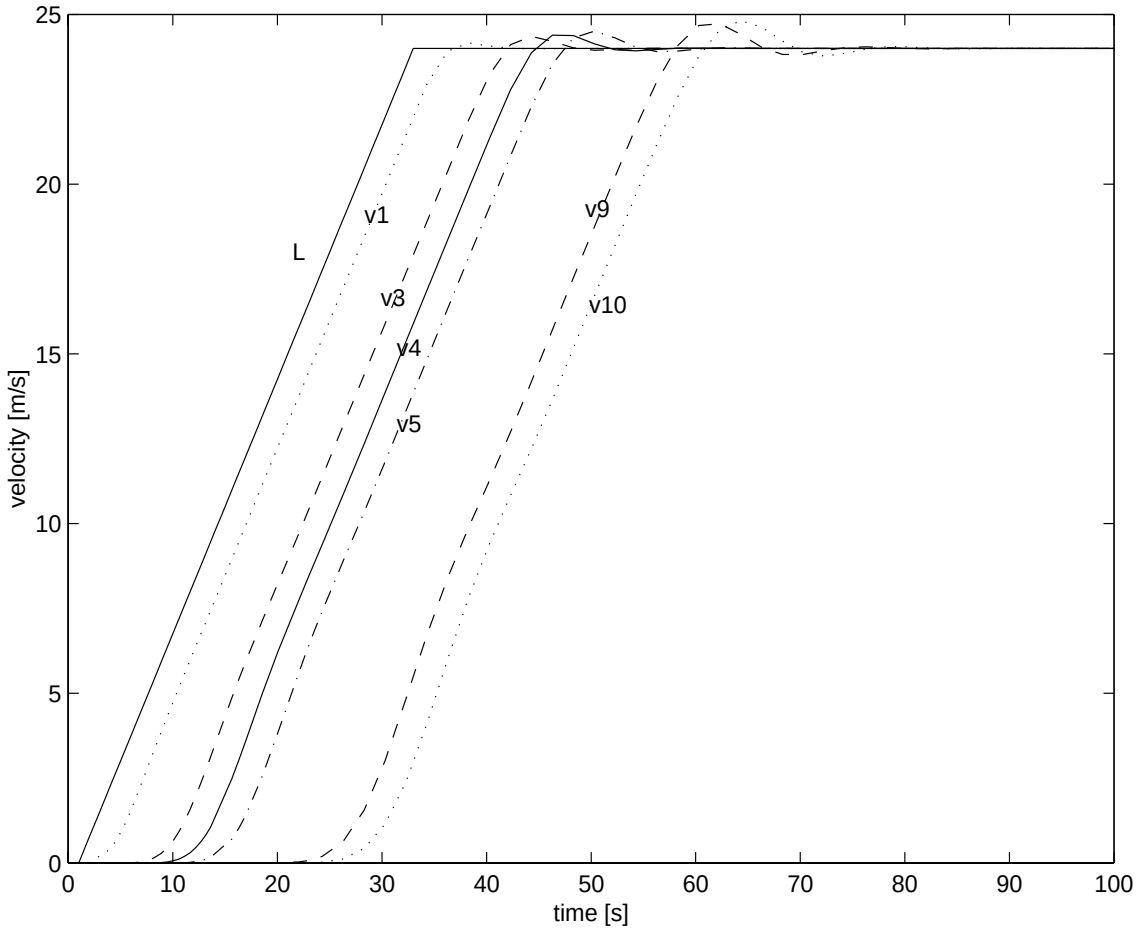

Figure 9(a): 10 vehicles in manual traffic (Pipes model) following a lead vehicle. Velocity response of leader (L), 1st vehicle (v1) and vehicles 3 to 5 (v3-v5) and 9,10 (v9, v10); (b)

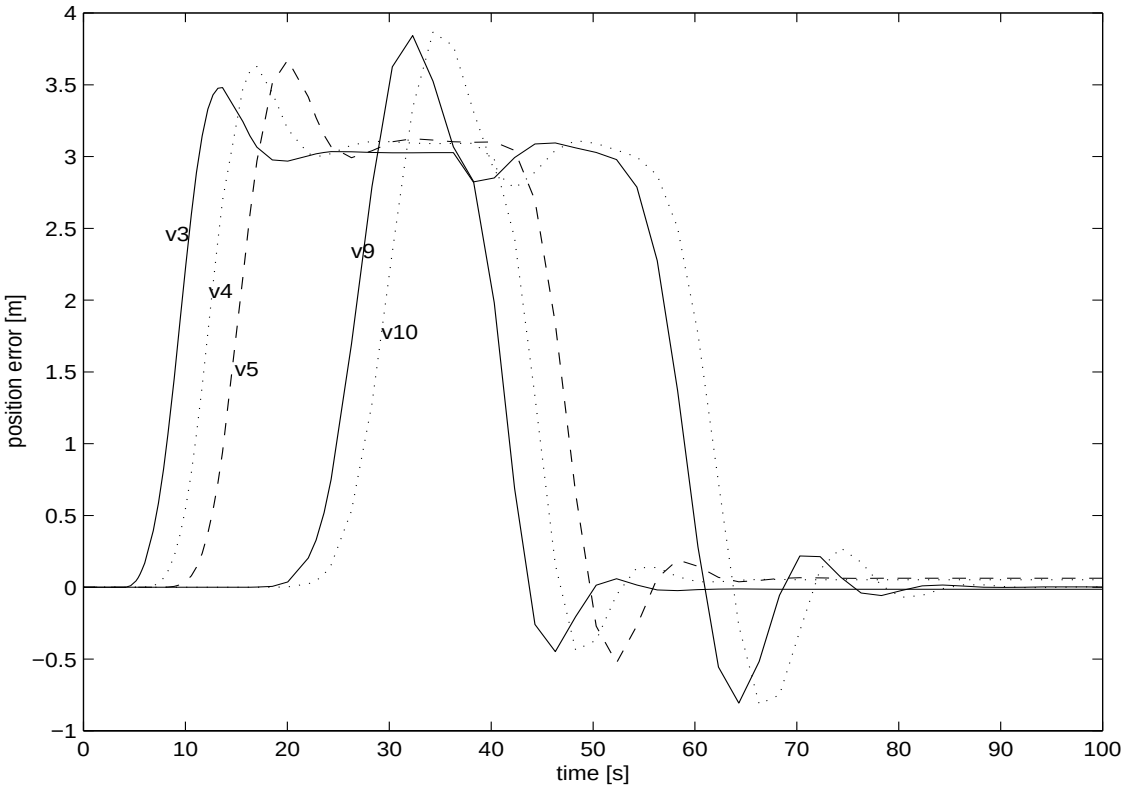

Figure 9(b): 10 vehicles in manual traffic (Pipes model) following a lead vehicle. position error of vehicles 3 to 5 (v3-v5) and 9,10 (v9, v10).

We now simulate different vehicle following scenarios in manual and mixed traffic. Since the objective is to study vehicle following transients, we do not investigate any safety aspects and assume normal vehicle operations with no instances of jeopardizing vehicle safety that might warrant emergency maneuvers.

For our case study, we examine the vehicle following transients in dense manual traffic where a string of 10 manually driven vehicles follow a lead vehicle in a single lane without passing. The lead vehicle accelerates from 0m/s to 24m/s with an acceleration of about 0.075g and the rest of the vehicles follow suit. Figure 9(a) shows the onset of slinky-type effect in the velocity responses of the following vehicles. We also observe in Fig. 9(b) that the position errors are amplified as they propagate upstream.

6.2 Mixed Traffic

Let us now consider a string of 10 vehicles following a lead vehicle in a single lane without passing in mixed manual/ICC traffic and examine the effect of mixing on the traffic flow characteristics during transients. The Pipes model, which is experimentally shown above to closely model the response of manually driven vehicles, is used for simulations. The validated ICC model presented in Section 4 is used to simulate ICC

vehicles. We consider the 4^{th} vehicle to be ICC, which corresponds to 10% mixing of ICC with manual vehicles. We consider two separate cases:

(i) Smooth acceleration by lead vehicle.

(ii) Rapid acceleration by lead vehicle.

(i) Smooth acceleration by lead vehicle

As an example consider the following situation. The lead vehicle accelerates smoothly from 0m/s to 24m/s at 0.075g and the rest follow suit. The velocity responses in Fig. 10(a) show good tracking by the ICC vehicle v4. It attenuates the position error and does not contribute to the slinky effect phenomenon as shown in Fig. 10(b). In this case because the ICC vehicle tracked very closely the response of the vehicle in front it did not affect the response of the manual vehicles upstream, as it is clear from Figure 9 and 10.

(ii) Rapid acceleration by lead vehicle

As an example consider the following situation. The lead vehicle accelerates at 0.35g from 0m/s to 24.5m/s, maintains a constant speed at 24.5m/s, thereafter decelerates to 14.5m/s at 0.3g and finally accelerates to 24.5m/s at 0.25g.
The simulated braking maneuver is such that it is a safe maneuver and a minimum vehicle spacing is always maintained for all vehicles. The velocity responses in Fig. 11(a) show that the ICC vehicle v4 filters the response of the rapidly accelerating vehicle v3 in an effort to maintain smooth driving. As a result the responses of vehicles v5, v9 and v10 are less oscillatory than that of v1 and v3. However, this is done at the expense of large position error in v4 (Fig. 11(b)).

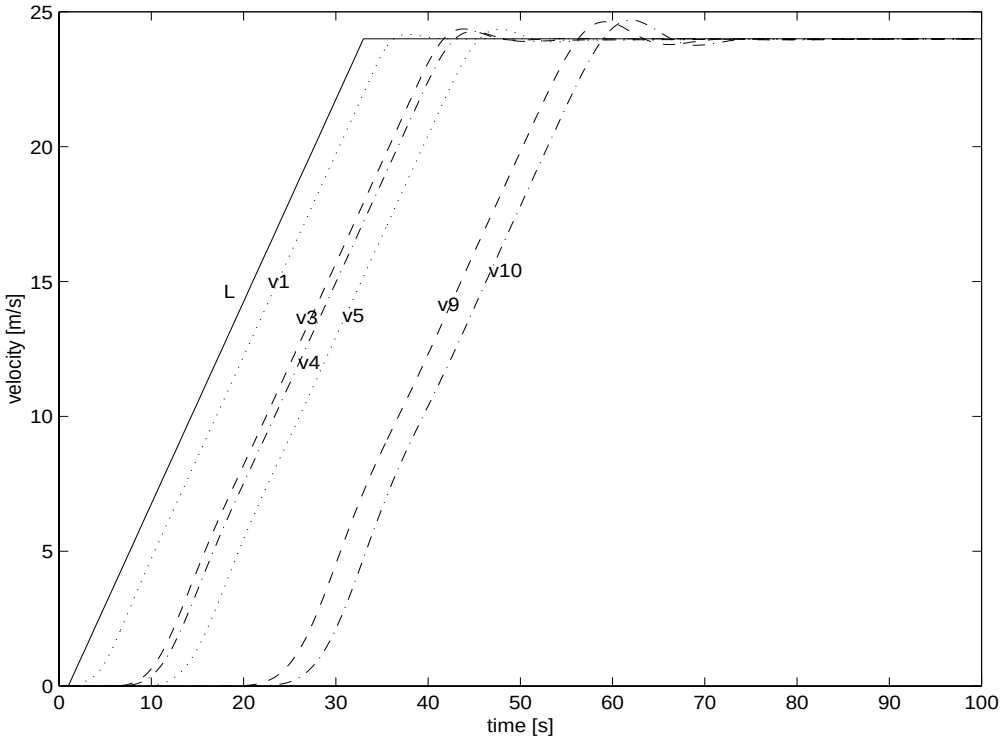

Figure 10(a): 10 vehicles in mixed manual (Pipes model)/ICC traffic following a lead vehicle performing smooth acceleration maneuvers. The 4th vehicle (v4) is ICC. Velocity response of leader (L), 1st vehicle (v1) and vehicles 3 to 5 (v3-v5) and 9,10 (v9, v10).

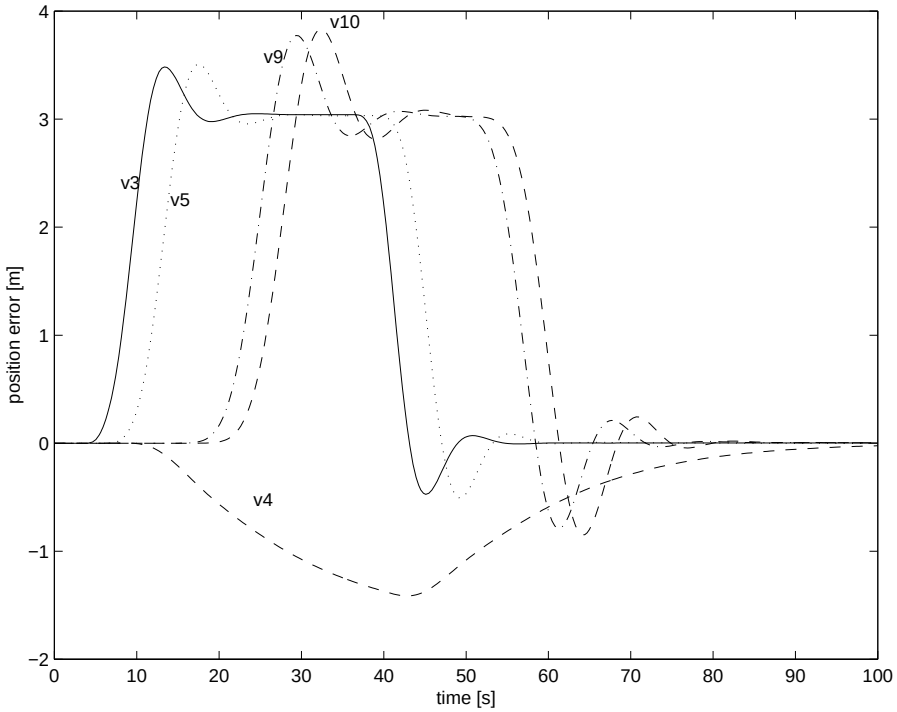

Figure 10(b): 10 vehicles in mixed manual (Pipes model)/ICC traffic following a lead vehicle performing smooth acceleration maneuvers. The 4th vehicle (v4) is ICC. position error of vehicles 3 to 5 (v3-v5) and 9,10 (v9, v10).

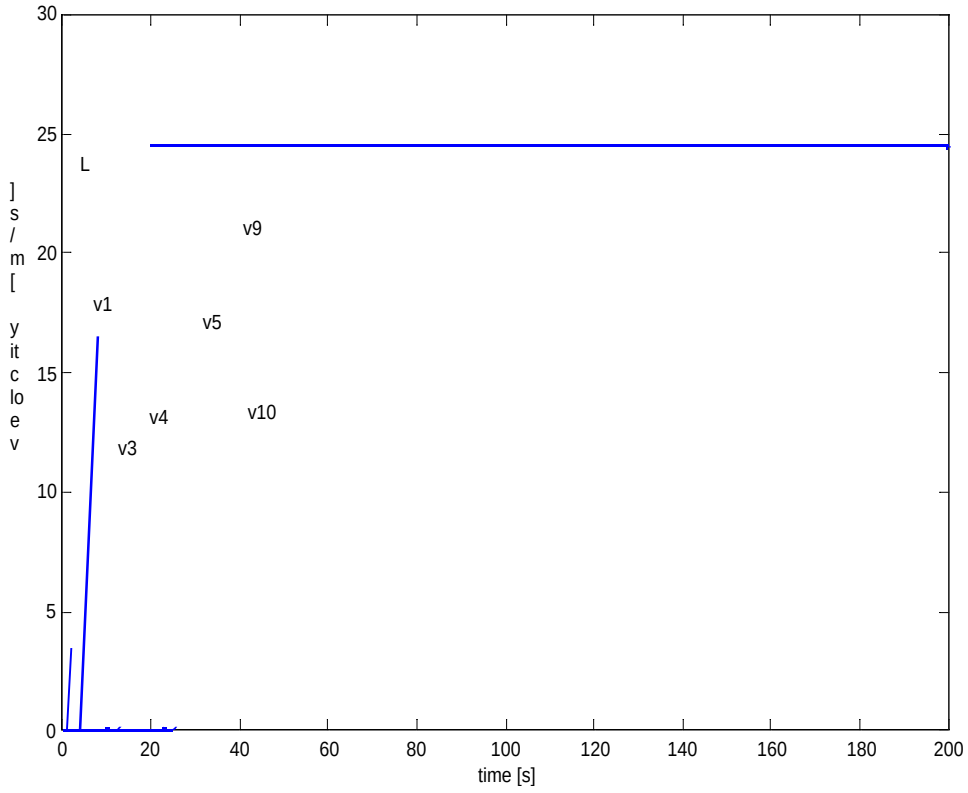

Figure 11 (a): 10 vehicles in mixed manual (Pipes model)/ICC traffic following a rapidly accelerating lead vehicle. The 4th vehicle (v4) is ICC. Velocity response of leader (L), 1st vehicle (v1) and vehicles 3 to 5 (v3-v5) and 9,10

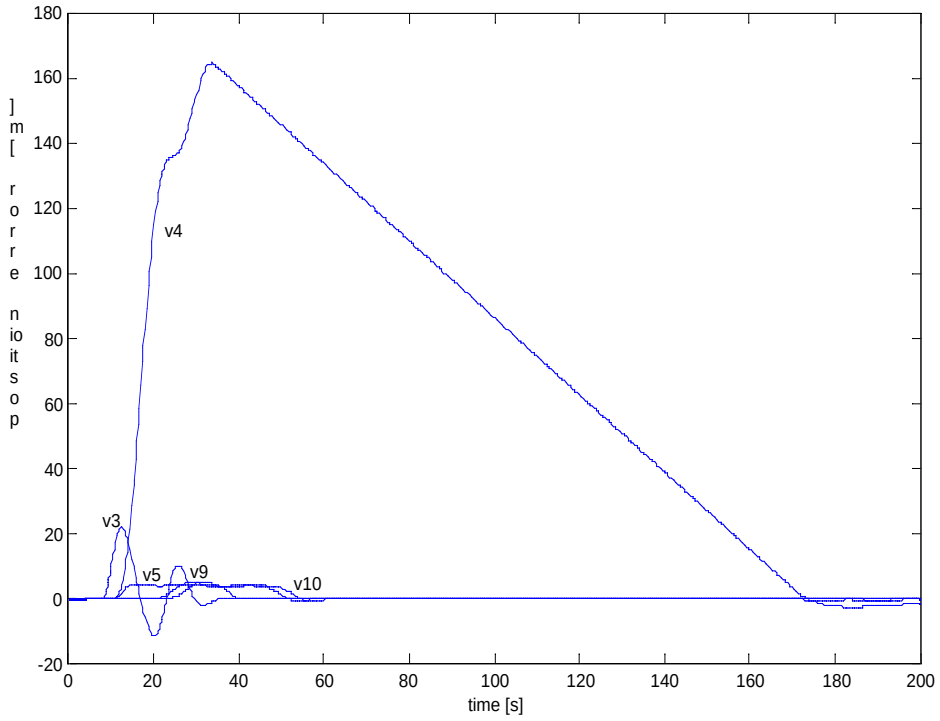

Figure 11 (b): 10 vehicles in mixed manual (Pipes model)/ICC traffic following a rapidly accelerating lead vehicle. The 4th vehicle (v4) is ICC. position error of vehicles 3 to 5 (v3-v5) and 9,10 (v9, v10).

7 Environmental Impact of Mixed Traffic

7.1 Introduction

In this Section we explore the benefits of ICC vehicles in mixed traffic in terms of pollution and fuel consumption. For traffic simulation models at the microscopic level, vehicle parameters such as second-by-second velocity, acceleration and grade for each individual vehicle determines the emission levels and fuel consumption [13]. For our simulation, we assume that the vehicles travel on a flat road with no change in grade and no wind gust. Secondary variables such as accessories like air-conditioning are neglected.

The quantities measured are the tailpipe emissions of unburnt hydrocarbons (HC), carbon monoxide (CO), CO_2, oxides of nitrogen (NO, NO_2, denoted by NO_x in this report) and fuel consumption. The Comprehensive Modal Emissions Model (CMEM) version 1.00 developed at UC Riverside is used to analyze the vehicle data and calculate the air pollution and fuel consumption [14]. It is a high fidelity, recently developed model that is more sensitive to transients than previous TRAF models [10]. The model calculates vehicle emissions and fuel consumption as a function of the vehicle operating mode, i.e. idle, steady state cruise, various levels of acceleration/deceleration, among others. The inputs to the software are two files: file-ctr and file-act. The first one is the control file that sets vehicle parameters such as units, secondary load, and vehicle category, among others. For our purpose, we use English units and category 5, i.e. high-mileage, high power-to-weight cars, which is the most common vehicle type in California. The second file records the vehicle activity. For our case, it is the recorded vehicle longitudinal speed. The outputs generated by the software are file-sbs and file-sum. The first one records the second-by-second tailpipe emissions of CO, HC, oxides of nitrogen (NO_x), CO_2 and fuel consumption. The second file gives a summary of these values for the trip.

7.2 Simulations

We examine the possible environmental benefits due to the presence of ICC vehicles in mixed traffic using the simulations in Section 6 for a string of 10 vehicles following a lead vehicle in a single lane without passing.

Smooth Acceleration

The lead vehicle accelerates smoothly from 0m/s to 24m/s at 0.075g and the rest follow suit. The total CO, CO_2, NO_x and HC emissions and fuel consumption by manual traffic are compared with that of mixed traffic in Fig. 12. It is seen that the accurate speed and position tracking of the ICC translates into lower air pollution and fuel savings as shown in Table 1.

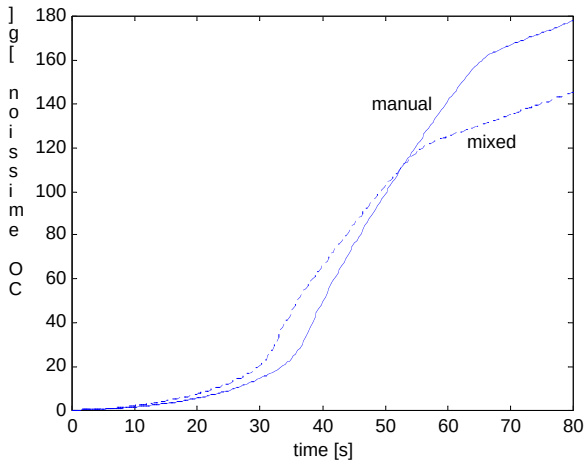

(a)

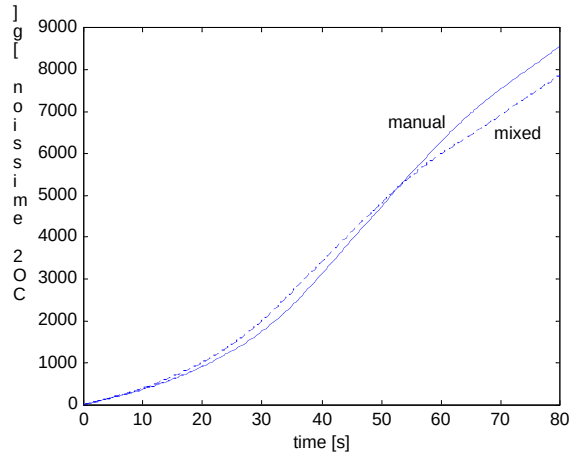

(b)

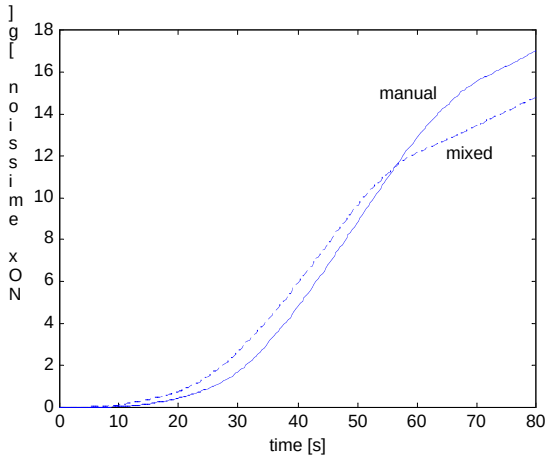

(c)

Figure 12: Comparisons between manual and mixed traffic for smooth acceleration maneuvers for cumulative (a) CO, (b) CO_2 and (c) NO_x emissions.

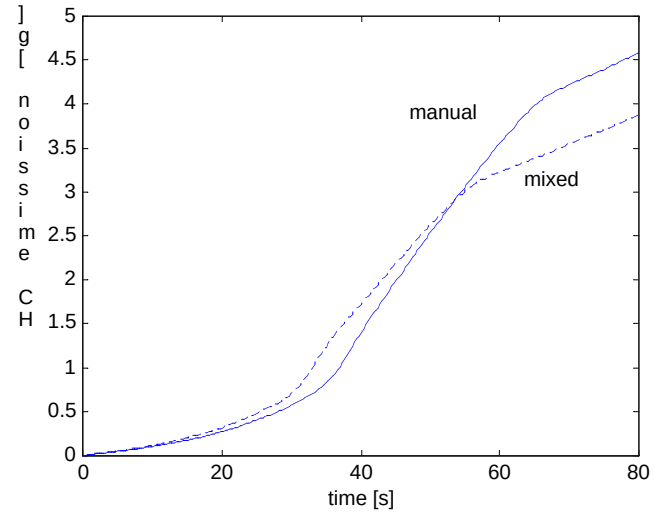

(d)

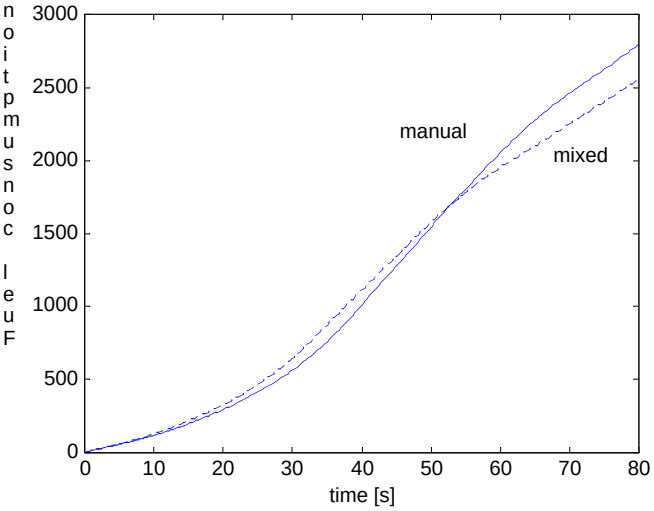

(e)

Figure 12: Comparisons between manual and mixed traffic for smooth acceleration maneuvers for cumulative (d) HC emissions and (e) fuel consumption.

Rapid Acceleration

When the lead manual vehicle performs rapid acceleration maneuvers as in Fig. 10, the pollution emissions and fuel consumption in manual traffic can be considerably reduced due to the presence of the ICC vehicle. Figure 13 shows the velocity responses of 6 vehicles in a string of 10 manually driven vehicles following a lead vehicle performing rapid acceleration maneuvers as in Fig. 11. The total CO, NO_x and HC emissions and fuel consumption by manual traffic (Fig. 13) are compared with that of mixed traffic (Fig. 11) in Fig. 14. The smoothing of traffic flow by the ICC vehicle significantly improves pollution levels and fuel consumption of manual traffic as indicated in Table 1.

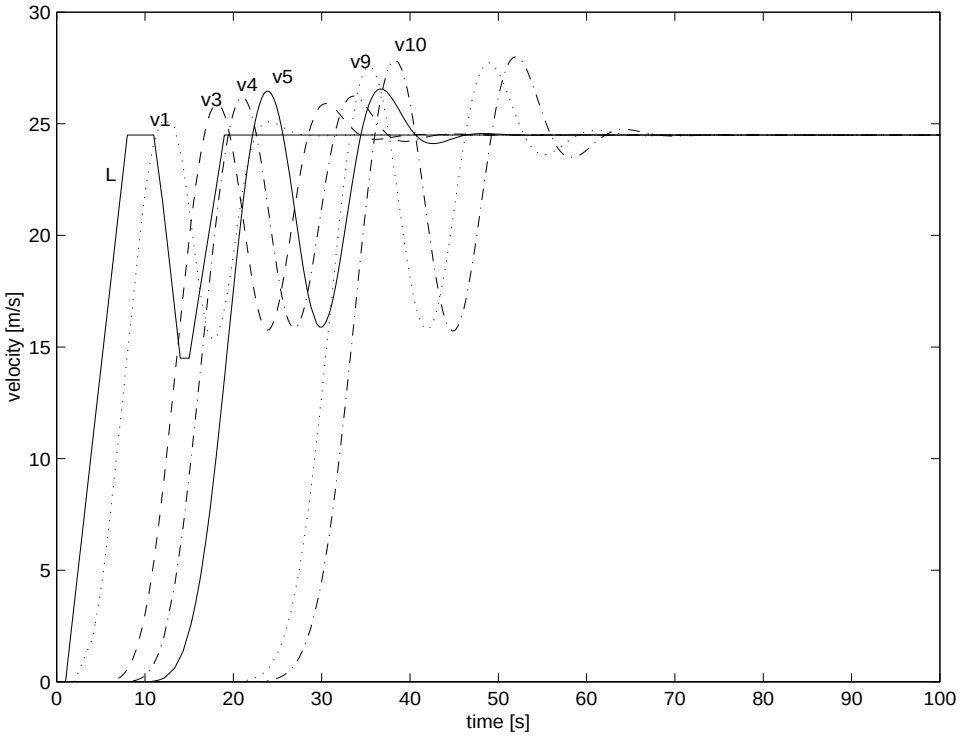

Figure 13: 10 manually driven vehicles follow a rapidly accelerating leader. Velocity response of leader (L), first vehicle (v1) and vehicles 3-5 (v3-v5) and 9,10 (v9, 10).

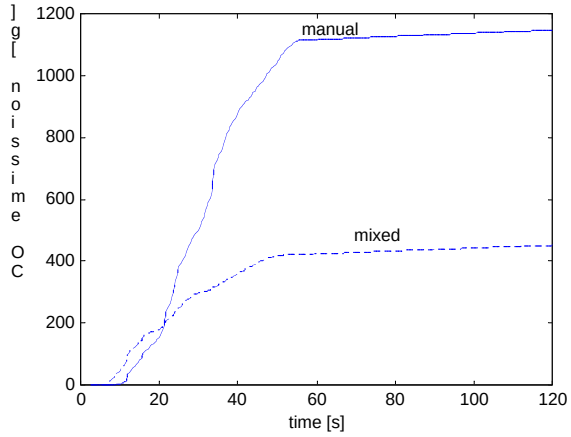

(a)

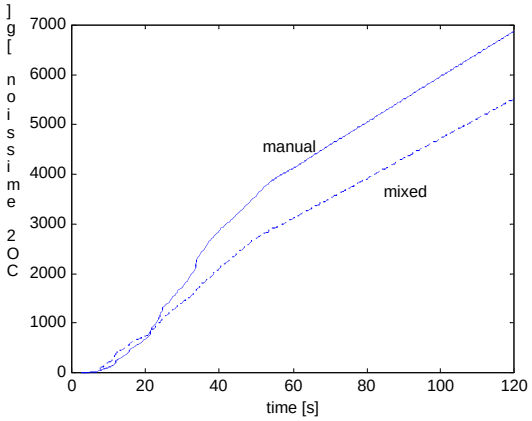

(b)

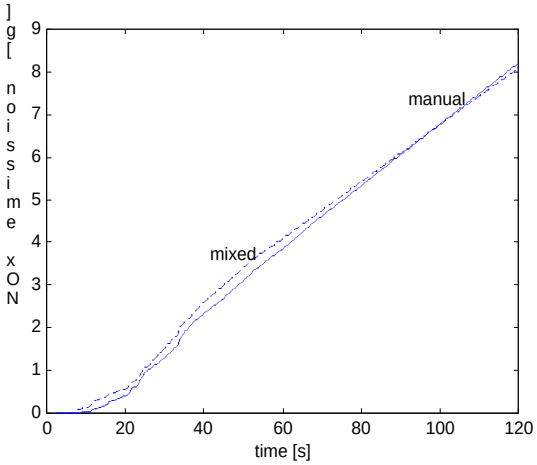

(c)

Figure 14: Comparisons between manual and mixed traffic for rapid acceleration maneuvers for cumulative(a) CO, (b) CO_2 , and (c) NO_x emissions.

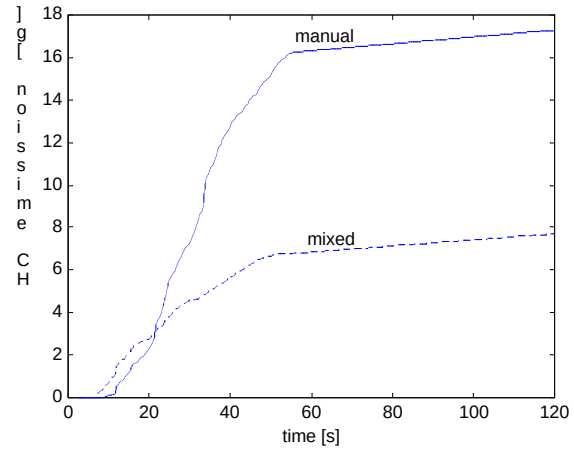

(d)

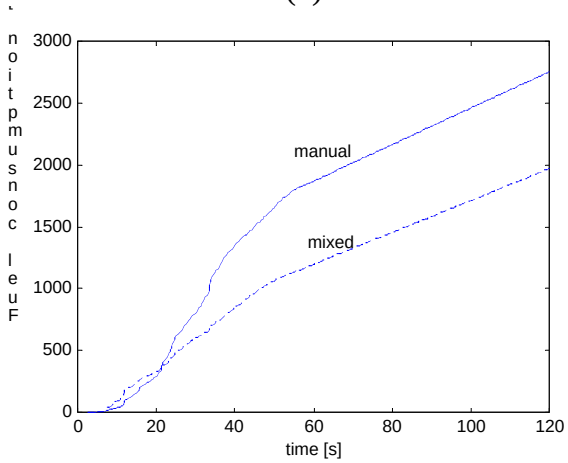

(e)

Figure 14: Comparisons between manual and mixed traffic for rapid acceleration maneuvers for cumulative (d) HC emissions and (e) fuel consumption.

	Smooth Acceleration	Rapid Acceleration
CO emission	18.4%	60.6%
CO_2 emission	8.1%	19.8%
NO_x emission	13.1%	1.5%
HC emission	15.5%	55.4%
Fuel consumption	8.5%	28.5%

Table 1: Percentage savings in cumulative pollution emission and fuel consumption for mixed traffic over manual traffic (simulation results).

7.2 Experiments

The aim is to perform experiments using actual vehicles to investigate the validity of the theoretical results developed in the previous Section. The experiments would be for two types of traffic – fully manual in which all vehicles are under manual control and mixed in which a single (ICC) vehicle is equipped with ICC system while the rest are manually driven. Three vehicles were used for the experiments, with one changing to ICC system for the mixed traffic scenarios.

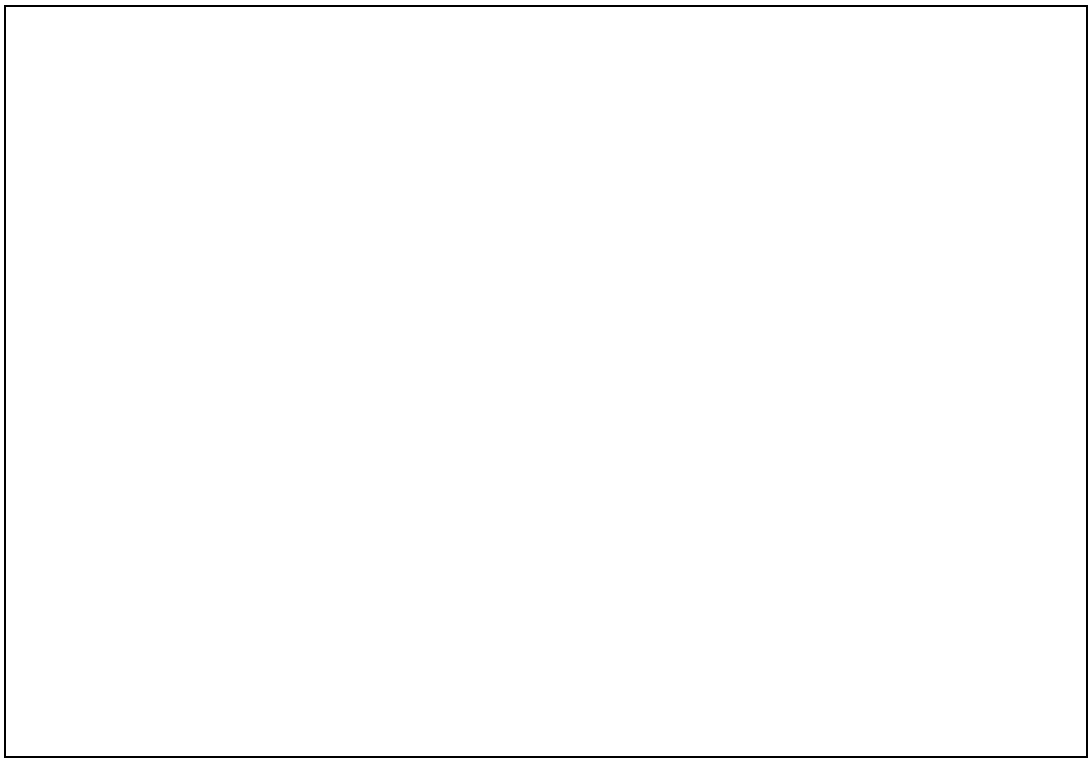

Figure 15: Experimental ICC vehicle.

The ICC software was implemented on a Ford Lincoln experimental vehicle shown in Fig. 15. The ICC controller uses range and range rate measurements from the forward-looking ranging sensor. However, due to noise corruption, no range rate data was available. So the algorithm was modified to do a differentiation of the range, taking the difference between the current range and the previous range over the time interval. This gave us a "pseudo range rate", albeit with a time delay. The variables that were recorded in the Ford Lincoln are: date/time stamp, vehicle spacing, longitudinal acceleration, desired longitudinal speed, actual longitudinal speed, desired throttle angle, actual throttle angle, desired brake pressure, actual brake pressure, position error, filtered time headway, brake on/off, range rate. The other two vehicles were Buick LeSabre and they were

equipped with data acquisition systems to record the speed and vehicle spacing, i.e. the distance to the lead vehicle if present. Details of the experiments are given in Appendix A.

For manual traffic, all vehicles were operated manually. The driver in the lead vehicle was instructed to follow a smooth speed profile to the best of his/her abilities. The drivers of the following vehicles responded by following the vehicle ahead with a comfortable headway. The vehicles were interchanged for different runs. For mixed traffic experiments, the ICC algorithm was implemented on the Ford Lincoln, which was used along with the two Buick LeSabres. A time headway of 1.0 sec was used in the ICC vehicle. The lead vehicle performed as closely as possible the same type of maneuvers as in manual traffic. The ICC (Ford) vehicle was placed as the second vehicle for the runs. The manual vehicles position was interchanged for different runs. The speed data collected from the experiments was analyzed using CMEM.

Three vehicles were used in the experiments since it was not possible to use 10 vehicles. Therefore to see how the simulation results compare with the experimental results, we reran the simulations using only 2 vehicles following a lead vehicle in manual traffic and mixed traffic. The lead vehicle speed profiles obtained during the experiments were used. The speed responses of the models were collected and analyzed using CMEM. The environmental benefits measured due to the presence of the ICC vehicle during experiments and simulations are presented in Table 2. The simulation results are conservative compared to environmental benefits in actual driving, a consequence of the fact that the Pipes model gives a smooth approximation of actual manual driving.

	Smooth Acceleration		Rapid Acceleration	
	Experiment	Simulation	Experiment	Simulation
CO emission	1.2%	0.8%	19.2%	12.3%
CO_2 emission	0.4%	0.2%	3.4%	3.3%
NO_x emission	1.6%	1.3%	25.7%	19.2%
HC emission	0.8%	0.4%	9.8%	6.6%
Fuel consumption	0.4%	0.2%	3.6%	3.4%

Table 2: Percentage savings in pollution emission and fuel consumption for mixed traffic over manual traffic.

8 Traffic Flow during the Presence of Rapid Acceleration Transients

In this Section we examine the effect of mixed traffic on the highway capacity and the traffic flow during transients and disturbances. Traffic flow is the number of vehicles passing a stationary observer on a highway measured per unit of time. Highway capacity is the theoretical maximum traffic flow on a highway without violating safety.

Theoretically, the percentage increase of ICC vehicles in mixed traffic increases the traffic flow at steady state conditions due to the smaller time headways used by the ICC vehicles [11]. The question, however, is whether the "sluggish" response of the ICC vehicles that is responsible for the environmental benefits shown in the previous Section affects traffic flow in the presence of traffic disturbances. We answer this question by performing the following simulations for manual and mixed traffic. Consider a stretch of road of length 2.5 km subdivided into 5 sections of 500m each. A constant traffic flow is assumed along the road. The manual vehicle dynamics are modeled using the Pipes linear car-following model from Section 3 and the ICC vehicle dynamics are modeled using the ICC design presented in Section 4. All vehicles follow a constant time headway policy. The time headways for the manual vehicles are generated according to a lognormal distribution given in [19] while for ICC vehicles they are taken as 1.0s. It is important to note that the time headway defined in [19] is the time taken to cover the distance that includes the vehicle length. The maximum value for the manual vehicle time headway is taken as 2.5s. This is done to make the study applicable to current manual traffic where a vehicle in moderately dense traffic conditions seldom uses a time headway greater than 2.5s. To calculate the traffic flow rate, we count the number of vehicles crossing a point of the highway. Assuming a detector at the end of section 5 on the road, we count the number of vehicles that cross the end of section 5 over a specified time interval and then average that to get the flow rate in veh/hr/lane. The specified measurement interval for traffic flow is taken to be 60secs. The simulation is run for 600secs that gives 10 measurements of traffic flow. We first consider manual traffic and then mixed traffic with 10% ICC vehicles. The ICC vehicles are placed randomly among the manually driven ones.

Initially all vehicles are travelling at 15m/s. Then after 60 sec when the first traffic flow count has been measured, the lead vehicle in section 5 accelerates away rapidly at 0.3g and the rest of the vehicles follow suit. In mixed traffic, if the lead vehicle in section 5 is an ICC vehicle, then it accelerates at its maximum value of 0.1g.

In Fig. 16(a) and 16(b) we plot the time headways of the vehicles on the highway at the start of the simulation in manual and mixed traffic, respectively. As seen, there are numerous manual vehicles with time headway 2.5 sec, since that is the stipulated upper limit. Also in Fig 16(b) the ICC vehicles can be seen with time headway of 1.0 sec. Fig 17 shows the traffic flow for the manual and mixed traffic. There is no significant effect of the rapid acceleration transients on the mixed traffic flow. This is so because transient phenomena do not affect the steady state traffic flow. The effect of the large vehicle spacing (and position error) of ICC vehicles is absorbed when aggregated over time. Furthermore, the average mixed traffic flow is greater than the manual traffic flow, as

expected. Moreover, Fig 18 shows the average traffic speed for each section. It increases from 15m/s after 60 sec when the lead vehicle in section 5 begins to rapidly accelerate. Also, some speed increase can be seen propagating over to section 4.

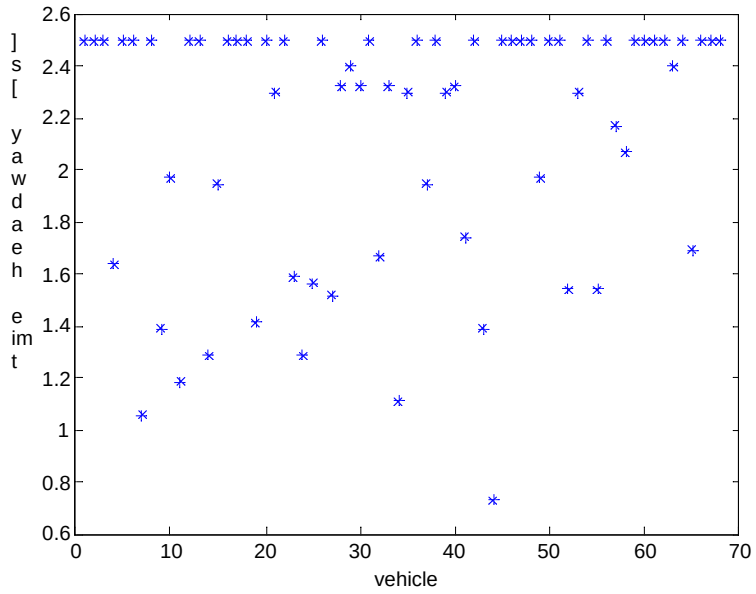

(a)

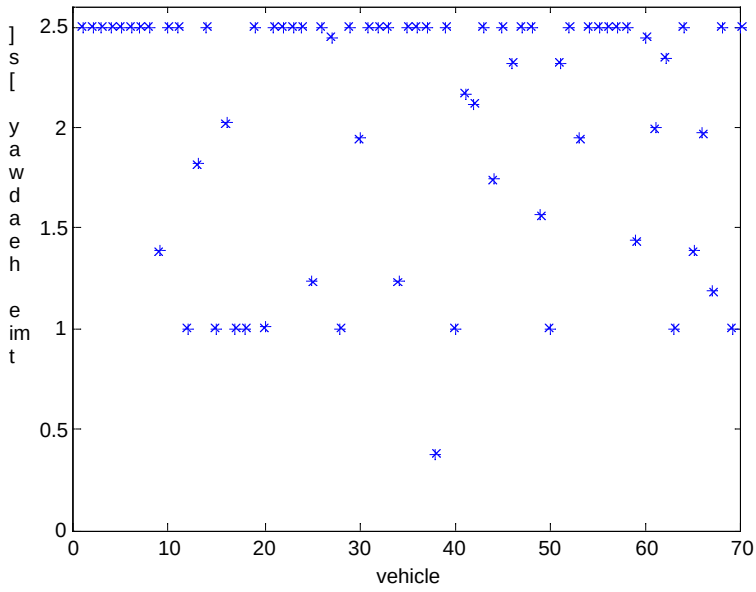

(b)

Figure 16: Time headway of vehicles at initial condition on a 2500m highway stretch during (a) manual and (b) mixed traffic.

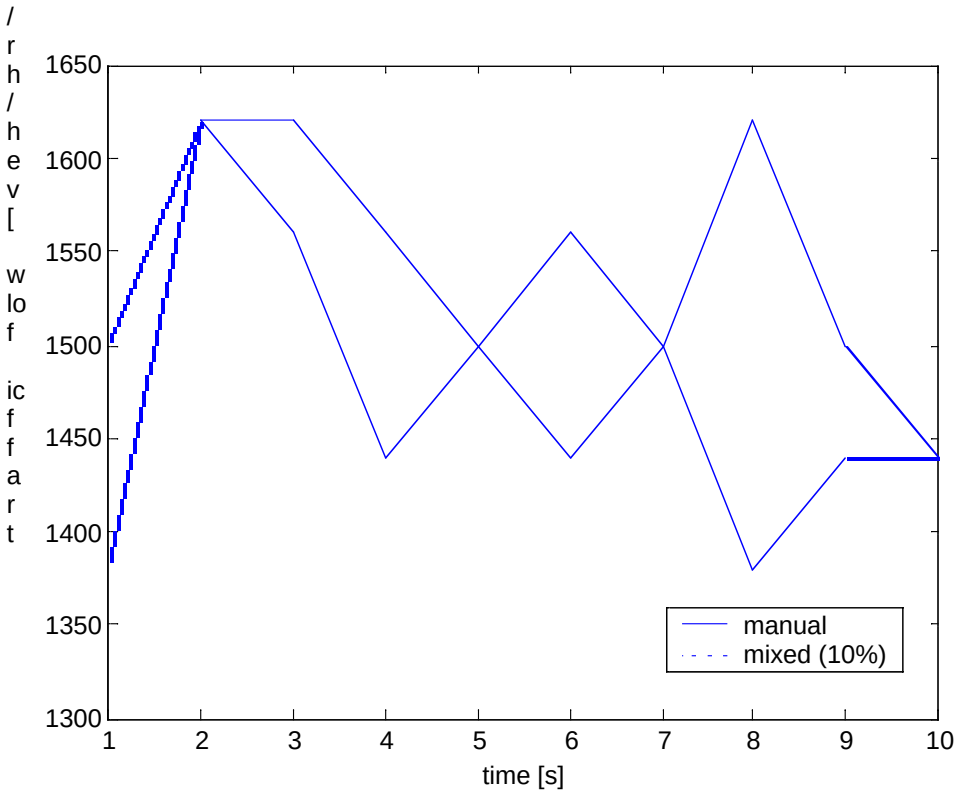

Figure 17: Traffic flow measured aggregated over 60 sec time intervals for manual and mixed traffic when the lead vehicle on the highway rapidly accelerates.

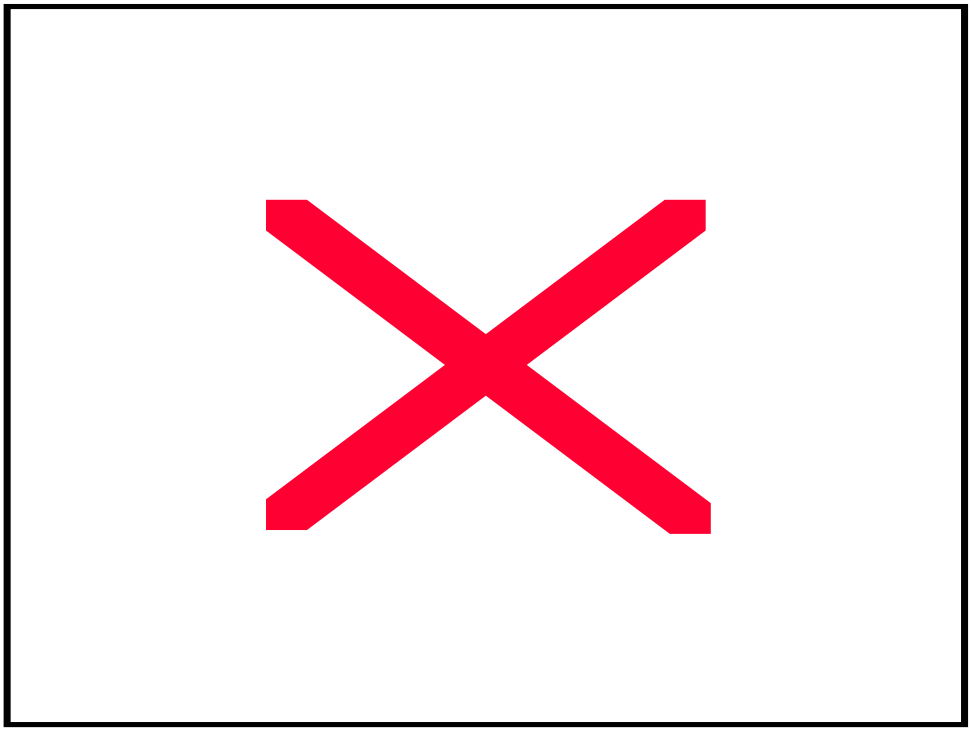

(a)

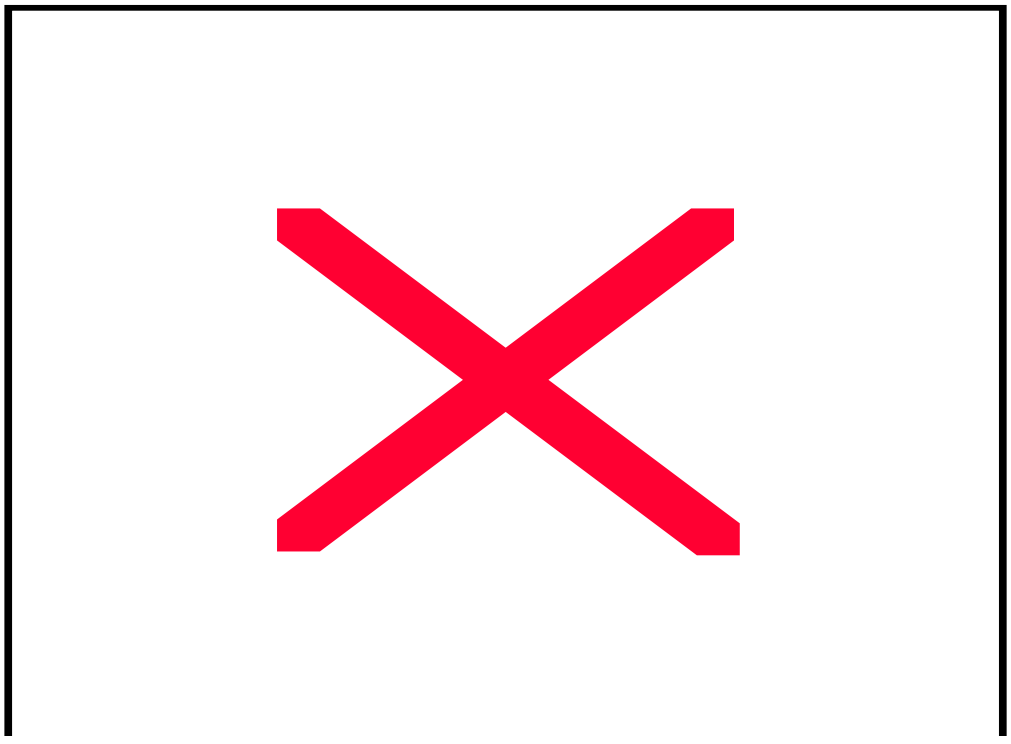

(b)

Figure 18: Average traffic speed in 5 sections in (a) manual and (b) mixed traffic when the lead vehicle in section 5 rapidly accelerates.

9 Conclusions

In this report we analyzed and simulated mixed manual/ICC traffic. Based on our findings, we can conclude the following:

- ICC vehicles in mixed traffic do not contribute to the slinky effect phenomena during smooth transients.

- ICC vehicles in mixed traffic smooth traffic flow by filtering the response of rapidly accelerating lead vehicles.

- The presence of ICC vehicles in mixed traffic improves air pollution levels and fuel savings during transients without adverse effects on the traffic flow rate.

References

[1] P. Ioannou and T. Xu, "Throttle and Brake Control", *IVHS Journal*, vol. 1(4), pp. 345-377, 1994.
[2] P. Ioannou and A. Bose, "Evaluation of Mixed Automated/Manual Traffic", USC CATT Report No. 97-09-10, September 1997.
[3] A. Bose and P. Ioannou, "Issues and Analysis of Mixed Semi-Automated/Manual Traffic", SAE Technical Paper Series No.981943, 1998.
[4] Consumers Reports Online, September 1998.
[5] M. J. Barth, "The Effect of AHS on the Environment", *Automated Highway Systems*, ed. P. Ioannou, Plenum Press, New York, 1997.
[6] S. Sheikholeslam and C. A. Desoer, "Longitudinal Control of a Platoon of Vehicles with no Communication of Lead Vehicle Information", *Proceedings of the 1991 American Control Conference*, Boston, MA, pp. 3102-3106.
[7] C. A. Desoer and M. Vidyasagar, *Feedback Systems: Input-Output Properties*, Academic Press Inc., New York, 1975.
[8] L. A. Pipes, "An Operational Analysis of Traffic Dynamics", *J. of Applied Physics*, vol.24, pp. 271-281, 1953.
[9] P. E. Chandler, R. Herman and E. W. Montroll, "Traffic Dynamics: Studies in Car Following", *Operations Research*, vol. 6, pp. 165-184, 1958.
[10] FHWA TRAF Simulation Model Emissions Maps.
[11] P. Ioannou and A. Bose, Automated Vehicle Control, *Handbook of Transportation Science*, Ed. Randolph Hall, pp. 187-232, Kluwer Academic Publishers, 1999.
[12] A. Bose and P. Ioannou, "Mixed Manual/Intelligent Cruise Control (ICC) Traffic Experiments", Draft Report, USC, 2000.
[13] M. J. Barth, "Integrating a Modal Emissions Model into Various Transportation Modeling Frameworks", *ASCE Conference Proceedings*, 1997.
[14] M.J. Barth, CMEM User's Manual, University of California, Riverside, 1998.
[15] R. J. Walker and C. J. Harris, "A Multi-Sensor Fusion System for a Laboratory Based Autonomous Vehicle", *Intelligent Autonomous Vehicles IFAC Workshop*, Southampton U.K., 1993, pp. 105-110

[16] *Special Report 209:* Highway Capacity Manual 1985, TRB, National Research Council, Washington D.C. 1985.
[17] D. Swaroop and J.K. Hendrick, “String Stability of Interconnected Systems”, *IEEE Trans. on Automatic Control,* vol. 41, No. 3, pp. 349-357, 1996.
[18] H. Raza and P. Ioannou, “Macroscopic Modeling of Automated Highway Systems" 36th IEEE Conference on Decision and Control, San Diego, California, Dec. 10-12, 1997, pp.4764-4770.
[19] S. Cohen, “Traffic Variables”, *Encyclopedia of Traffic Flow*, Ed. M. Papageorgiou. Pp.139-143.
[20] P. Ioannou and T. Xu, “Throttle Control for Vehicle Following”, USC Report 92-11-02, November, 1992.

Appendix A: Experiments using Actual Vehicles

A.1 Test Set-up & Software Implementation

The aim was to perform experiments using actual vehicles. The experiments would be for two types of traffic – fully manual in which all vehicles are under manual control and mixed in which a single vehicle is equipped with ICC system while the rest are manually driven. Three vehicles were used for the experiments, with one changing to ICC system for the mixed traffic scenarios.

Simulation Model

It was necessary to have a Data Acquisition System in all vehicles to record their speed and vehicle spacings (for vehicles #2 and #3). The ICC controller was to be implemented on a Ford Lincoln Continental that was equipped with a frontal looking ranging sensor. The software to be implemented was designed and tested at USC. For the testing, a vehicle model was obtained from Ford Motor Co. This model is validated for high gear freeway driving. The model vehicle dynamics is given by

$$\dot{v} = \frac{1}{EffectiveInertia}\left\{Brake/Engine\_Torque - R_w(F_{rr} + 0.44v^2)\right\}$$

where

v is the vehicle speed
EffectiveInertia is the vehicle Inertia
Brake/Engine_Torque is the torque when the throttle or brake is active
R_w is the radius of wheel
F_{rr} is the rolling resistance

The throttle input to the model is Mark Space Ratio (MSR) where 15 MSR and 80 MSR correspond to closed (0.0 degree) and open (85.0 degrees) throttle, respectively. The brake pressure input is given in bar. However, the experimental Ford vehicle uses degrees and psi as throttle and brake inputs, respectively. While conversion from psi to bar involves a factor of 1/14.69, the conversion from degrees to MSR is not trivial. First, a mapping was made for MSR-to-vehicle speed. Second, a throttle-to-vehicle speed mapping from [20] was used. This enabled us to develop a mapping from degree-to-MSR. To ensure that the mapping is correct, we developed a mapping from throttle to speed using simultaneously throttle-to-MSR and MSR-to-speed mappings and compared it to the original from [20]. As can be seen in Fig. A-1, it gave good mapping results. So the designed algorithm gave throttle and brake commands in degrees and psi, respectively, as it would in the Ford vehicle. In the simulation, the throttle command in degrees was mapped to vehicle speed that was mapped to MSR and the brake command in psi was converted to bar.

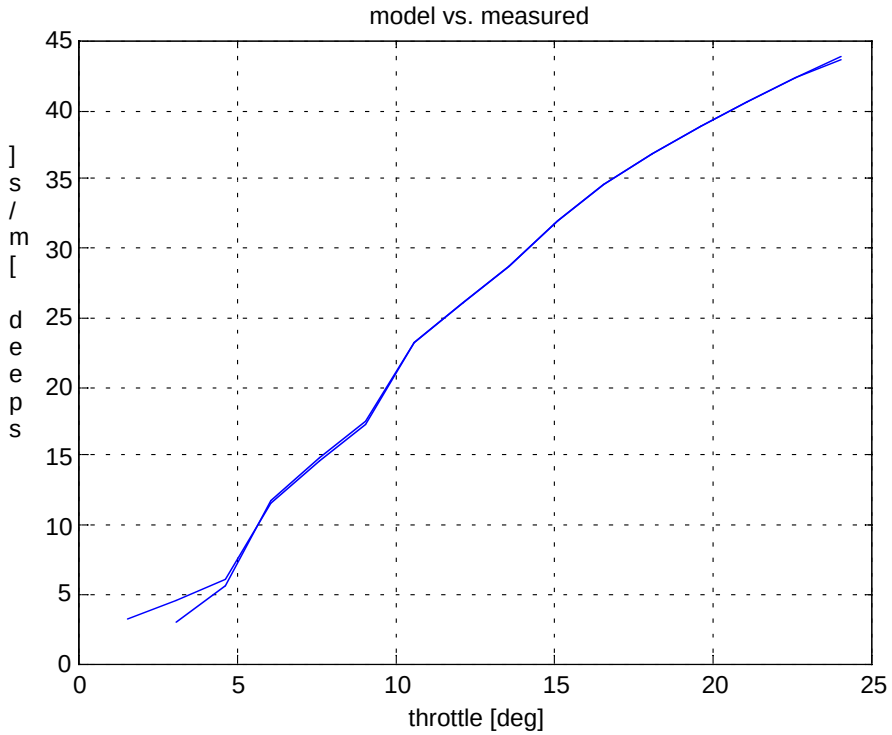

Figure A-1: Throttle-to-speed mapping for vehicle model.

Experimental Vehicles

The ICC software designed and tested using the model described above was implemented on the Ford Lincoln experimental vehicle shown in Fig 3. The computer in the Ford uses QNX operating system on a rugged zed 33 MHz 80486 Computer with 8 MB of memory. The forward looking ranging sensor is a 24 GHz radar from O'Conner Engineering using Frequency Modulated Continuous Wave (FMCW) for range and having a maximum range of 30m. The throttle actuator is a stepper motor while a hydraulic booster is used for the brake actuator. The QNX provides Unix model tasking and development environment with real-time response. It takes care of the communication and integrates the device drivers with the program modules.

Figure A-2 depicts the software environment for the Ford vehicle. Inputs to the software are readings from the longitudinal sensors and radar data. The output commands are for the throttle and brake actuators. In addition, there are two meters mounted on the dashboard that are used to display variables. The Ford vehicle can use vehicle-to-vehicle communication but in our mixed traffic application this is not used, hence we shall not refer to it. Figure A-3 shows the three communicating processes. Processes communicate with each other by passing data structures to a globally shared database. The main program module is called eng_spd.c which implements an interface for engine control using the

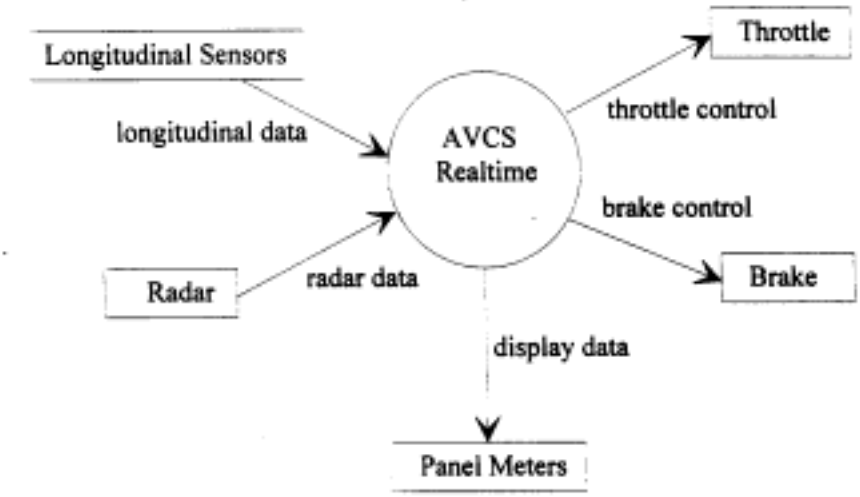

Figure A-2: Software environment in the ICC vehicle.

longitudinal AVCS system. It interacts with module veh_io.c as shown in the figure. This module contains vehicle specific configurations and hardware I/O transformations for AVCS control. It sets up vehicle parameters from a configuration file, reads the hardware device drivers ATMIO-16 and PCTIO-10, stores the information in the database and writes to ATMIO-16 and PATH-101 as shown in Fig A-4.

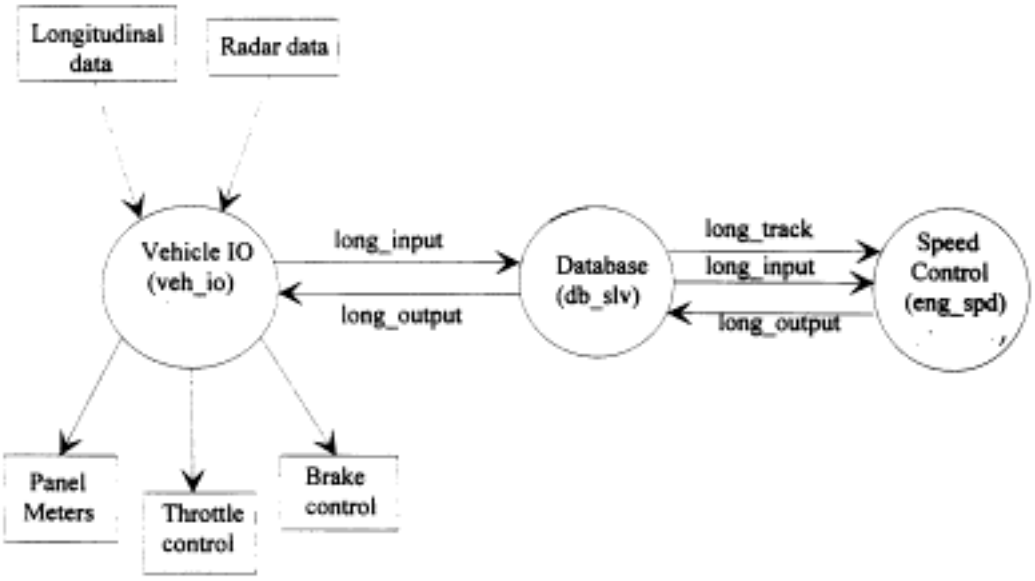

Figure A-3: AVCS real-time in the ICC vehicle.

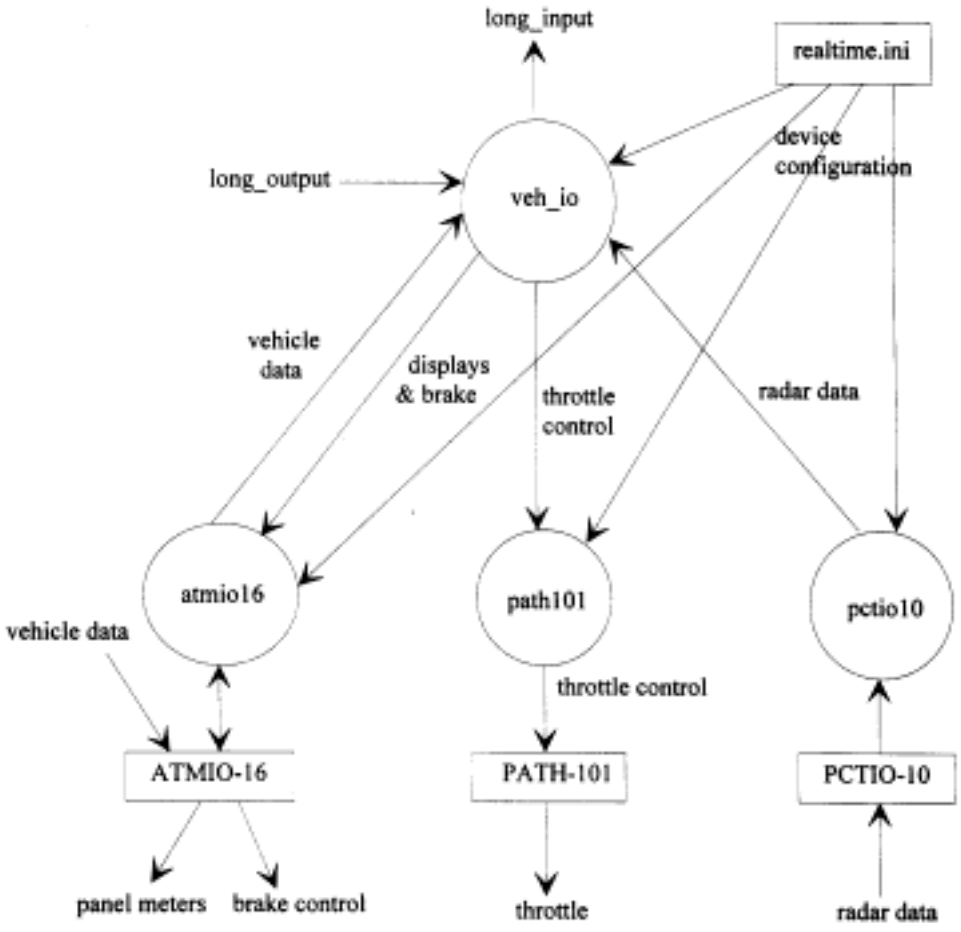

Figure A-4: Vehicle input-output in the ICC vehicle.

The eng_spd.c modules has three functions: spd_init( ), spd_ctrl( ) and spd_done( ) as shown in Fig A-5. Their functions are:

- spd_init ( ): routine is called when the controller first starts and contains all run-time initializations for the controller configuration and static initializations for the filters.
- spd_ctrl ( ): routine called by AVCS every 20 msec when new vehicle data is available. Performs all control calculations and sets the desired throttle and brake control outputs.
- spd_done ( ): routine called when the controller exits. Cleans up resources allocated by spd_init ( ) and spd_ctrl ( ) functions.

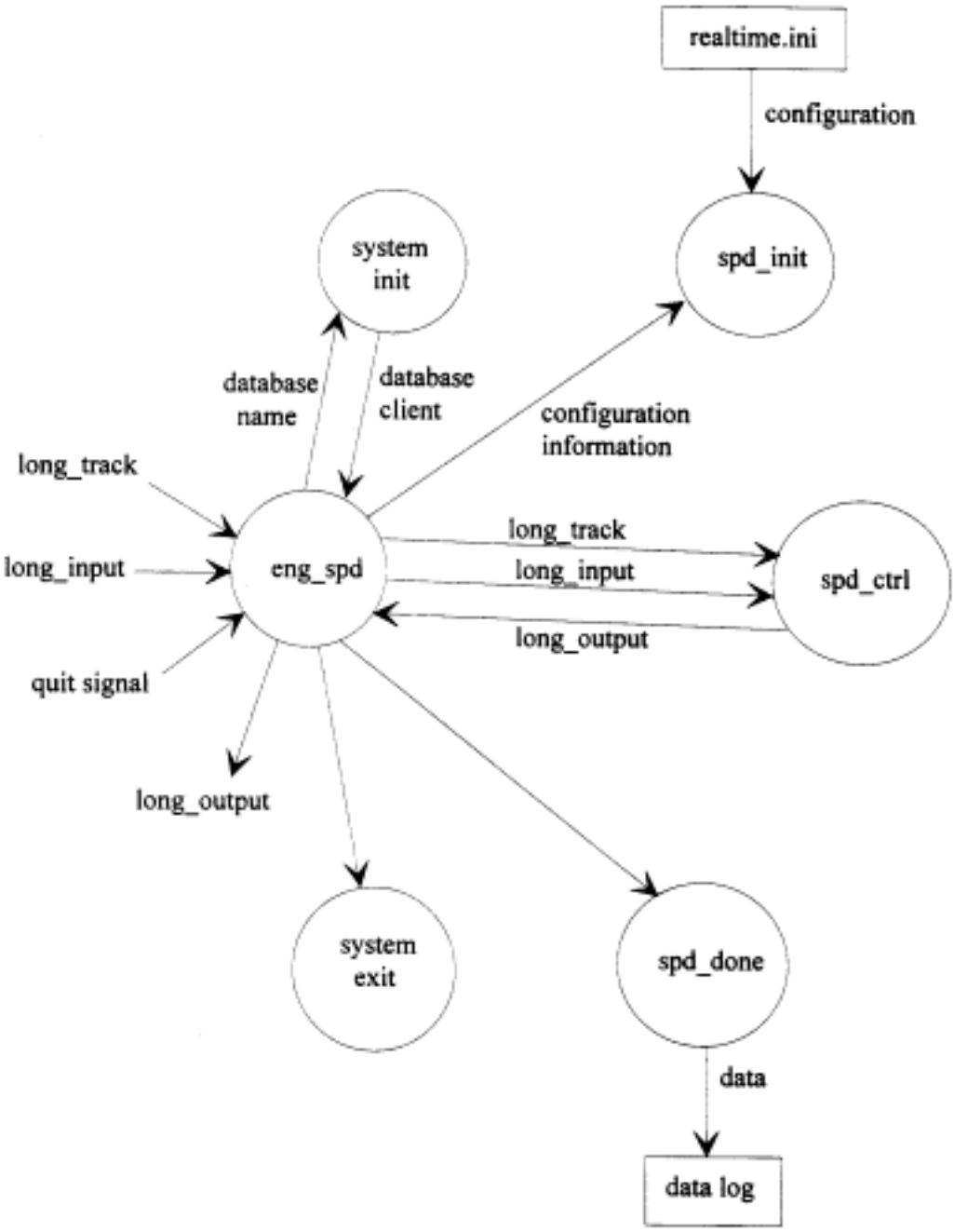

Figure A-5: Speed control in the ICC vehicle.

The ICC controller uses range and range rate measurements from the forward-looking ranging sensor. However, due to noise corruption, no range rate data was available. So the algorithm was modified to do a differentiation of the range, taking the difference between the current range and the previous range over the time interval. This gave us a “pseudo range rate”, albeit with a time delay. The variables that were recorded in the Ford Lincoln are: date/time stamp, vehicle spacing, longitudinal acceleration, desired

longitudinal speed, actual longitudinal speed, desired throttle angle, actual throttle angle, desired brake pressure, actual brake pressure, position error, filtered time headway, brake on/off, range rate. The other two vehicles are Buick LeSabre and they are equipped with DAS to record the speed and vehicle spacing, i.e. the distance to the lead vehicle if present.

A.2 Experiments

The experiments were performed at a former Navy base at Crow's Landing. The three vehicles were run on a runway strip approximately 1.5 miles in length.

Validation

The model outlined in the previous section was validated using step inputs for the throttle and the brake controller in the experimental vehicle. The least count of the speedometer of the Ford Lincoln is 1 mph. The results indicate that the model agrees with the experimental vehicle.

Throttle angle [degrees]	Vehicle Speed [mph]	
	Simulation	Experiment
6.0	26.3	28
7.5	33.2	32
9.0	38.6	38
10.5	51.3	48
12.0	57.8	57

Table A-1: Validation of the throttle subsystem.

The brake actuator validation was performed as follows: after cruising at a speed, the brakes were applied. The time taken to come to a complete stop was recorded, and thus deceleration was calculated.

Brake Pressure [psi]	Deceleration [m/s^2]	
	Simulation	Experiment
150	-1.1	-1.4
200	-1.5	-1.8
250	-2.5	-2.33
300	-2.75	-2.78
350	-3.0	-3.1

Table A-2: Validation of the brake subsystem.

The simulation model is very close to the experimental vehicle, as seen in Tables 1 and 2.

4.2 Vehicle following in Manual and Mixed Traffic

A time headway of 1.0 sec was used in the ICC vehicle. For manual traffic, all vehicles were operated manually. The driver in the lead vehicle was instructed to follow a smooth speed profile to the best of his/her abilities. Drivers of the following vehicles responded by trying to follow the vehicle ahead with a comfortable headway. The vehicles were interchanged for the same set of runs. For mixed traffic experiments, the ICC algorithm was implemented on the Ford Lincoln which was used along with the two Buick LeSabres. The lead vehicle performed the same type of maneuvers as in manual traffic. The ICC (Ford) vehicle was placed as the second vehicle for the runs.

The speed and acceleration responses of three manually driven vehicles following smooth acceleration speed profiles are shown in Fig. A-6 and Fig.A-7, respectively. The speed and acceleration response of the ICC vehicle and the two manually driven vehicles following smooth acceleration speed profiles are shown in Fig. A-8 and Fig. A-9, respectively. The position error of the ICC vehicle is shown in Fig. A-10. The desired and actual throttle angle of the ICC vehicle are shown in Fig. A-11 and the desired and actual brake command in Fig. A-12. As observed in Fig. A-11, when the brake is on and the desired throttle angle is zero, the actual throttle angle is set to it minimum value of about 1°. Moreover, Fig. A-12 shows that the brake actuator has some backlash error and does not go back to 0 psi after turning off [21].

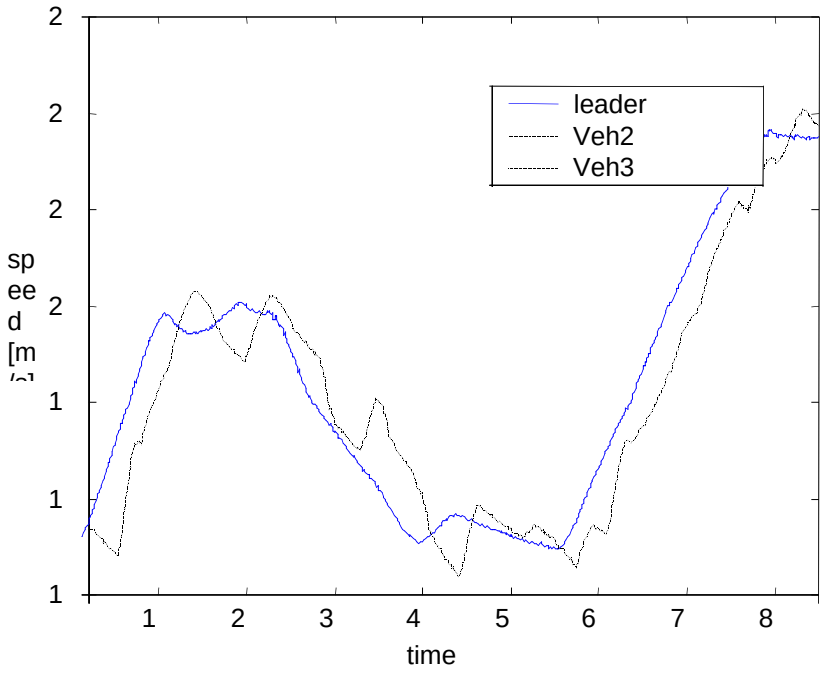

Figure A-6: Speed responses of three manually driven vehicles during smooth accleration manuvers.

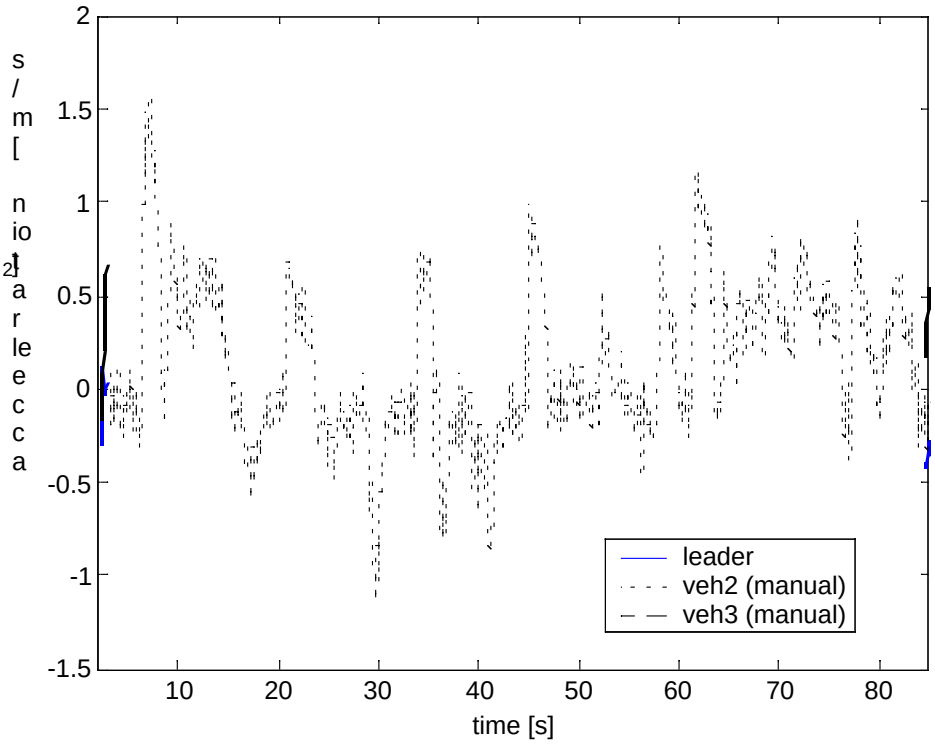

Figure A-7: Acceleration of three manually driven vehicles during smooth accleration manuvers.

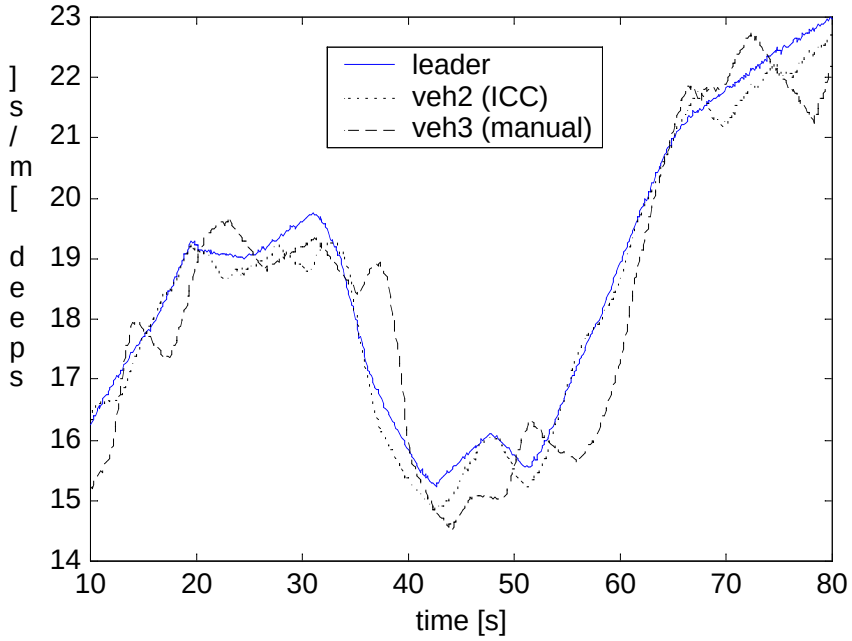

Figure A-8: Speed responses of two manually driven vehicles and an ICC vehicle between them during smooth accleration manuvers.

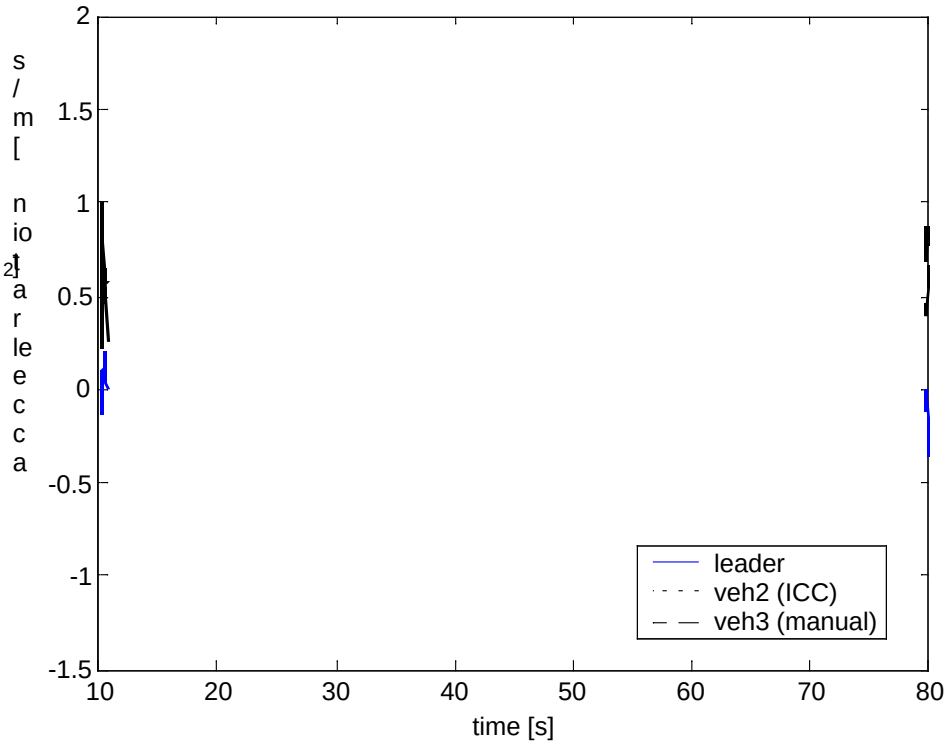

Figure A-9: Acceleration of two manually driven vehicles and an ICC vehicle between them during smooth acceleration manuvers.

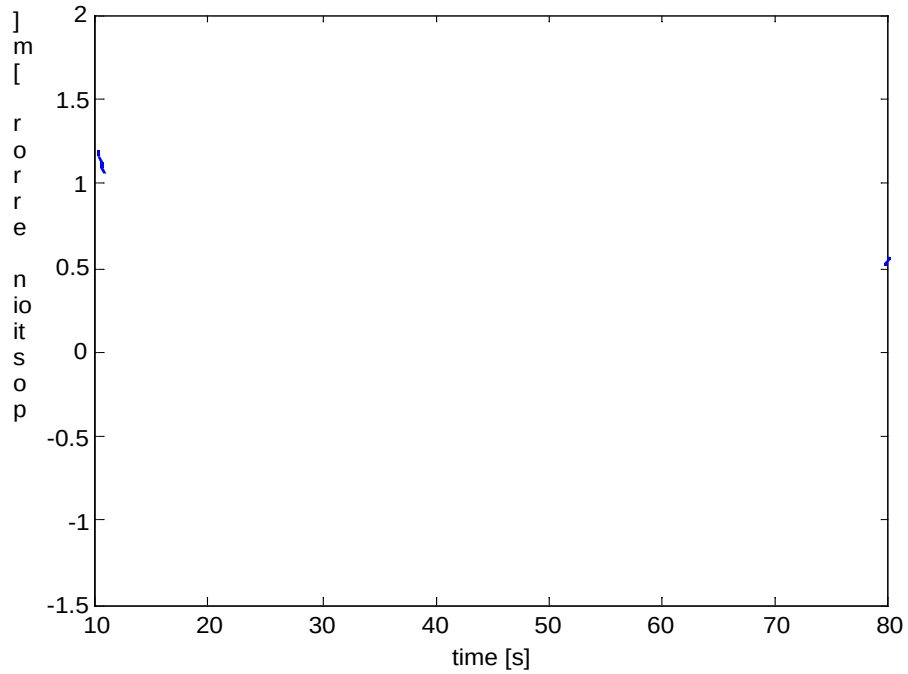

Figure A-10: Position error in the ICC vehicle during smooth acceleration maneuvers.

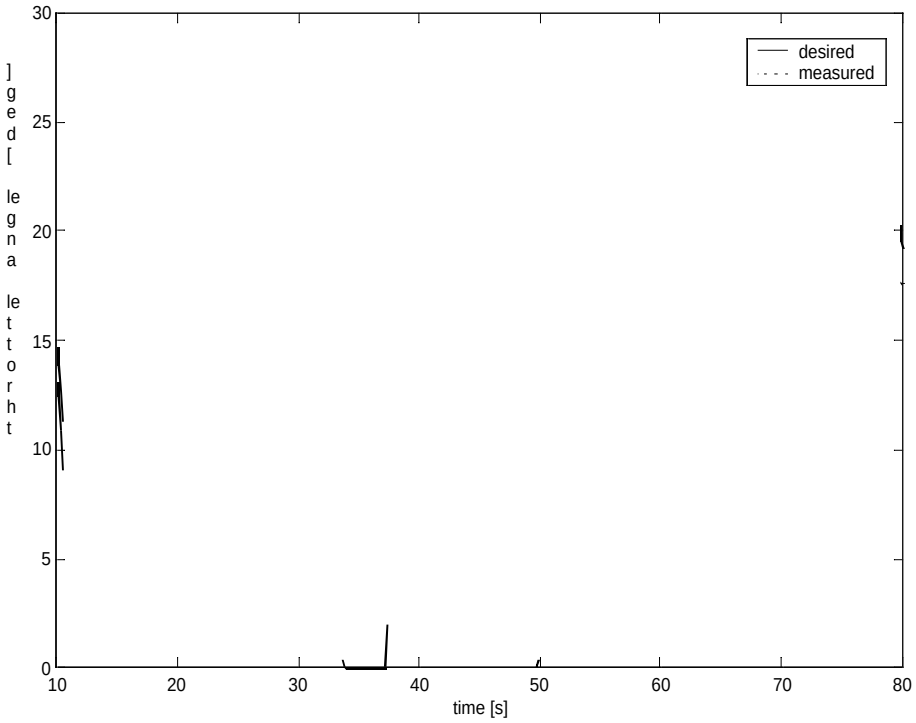

Figure A-11: The desired and actual throttle angle of the ICC vehicle during smooth accleration manuvers.

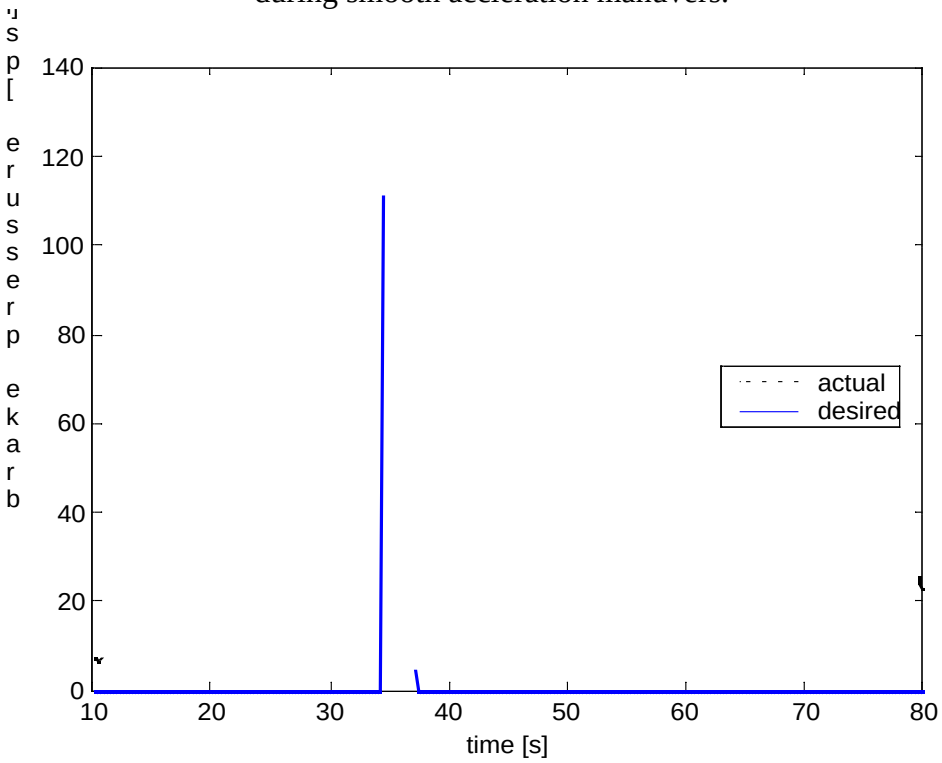

Figure A-12: The desired and actual brake line pressure of the ICC vehicle during smooth accleration manuvers.

The authors wish to thank PATH researchers Benedict Bougler, David Nelson and Xiao-Yun Lu for their discussions and help in driving the vehicles (Fig. A-13).

Figure A-13: PATH researchers, one of the authors and the ICC vehicle at the experiment site.